GEOCHEMICAL CONTROLS ON ARSENIC, URANIUM AND MOLYBDENUM MOBILITY IN A LOW-LEVEL RADIOACTIVE WASTE MANAGEMENT AREA IN ONTARIO, CANADA

A Thesis Submitted to the College of Graduate and Postdoctoral Studies

In Partial Fulfillment of the Requirements

For the Degree of Master of Science

In the Department of Geological Sciences

University of Saskatchewan

Saskatoon

By

DANIELLE RENEE VEIKLE

PERMISSION TO USE

In presenting this thesis in partial fulfilment of the requirements for a Postgraduate degree from the University of Saskatchewan, I agree that the Libraries of this University may make it freely available for inspection. I further agree that permission for copying of this thesis in any manner, in whole or in part, for scholarly purposes may be granted by the professor or professors who supervised my thesis work or, in their absence, by the Head of the Department or the Dean of the College in which my thesis work was done. It is understood that any copying or publication or use of this thesis or parts thereof for financial gain shall not be allowed without my written permission. It is also understood that due recognition shall be given to me and to the University of Saskatchewan in any scholarly use which may be made of any material in my thesis.

Requests for permission to copy or to make other use of material in this thesis in whole or part should be addressed to:

Head of the Department of Geological Sciences
114 Science Place
University of Saskatchewan
Saskatoon, Saskatchewan S7N 5E2

OR

Dean
College of Graduate and Postdoctoral Studies
University of Saskatchewan
116 – 110 Science Place
Saskatoon SK S7N 5C9

ABSTRACT

Contaminant leaching from industrial wastes can have widespread negative impacts on water quality, ecosystem processes, and human health. Low-level radioactive wastes derived from uranium (U) ore processing contain several potentially-hazardous metal(loid)s including U, arsenic (As) and molybdenum (Mo). Predicting the release, transport and attenuation of these and other contaminants is challenging due to complex geochemical behaviour impacting their mobility in soils, sediments and groundwater. The release, transport and attenuation of U, As and Mo in these systems is strongly controlled by pH and redox conditions, which influence both aqueous speciation and mineral solubility.

Research was conducted to examine geochemical controls on As, U and Mo mobility within soil contaminated with low-level radioactive waste stored in Waste Management Area F (WMAF) at Chalk River Laboratories (Chalk River, Ontario, Canada). Core samples were collected as a function of depth at several locations in WMAF. Geochemical and mineralogical characteristics of these samples was examined and a subset of samples containing elevated concentrations As, U and Mo was selected for additional study. Sequential extractions and synchrotron-based X-ray absorption near edge structure (XANES) spectroscopy identified major forms As, U and Mo present in this subset of samples. Column experiments were conducted to examine release of these elements under anoxic and oxic conditions. Batch experiments were performed to quantify potential for As, U and Mo attenuation by sediments underlying WMAF.

Results demonstrated that As and U release are strongly controlled by redox conditions and Mo is strongly controlled by pH. In general, As release was greatest under anoxic conditions, while U release was greatest under oxic conditions. In contrast, elevated Mo concentration were observed in leachates generated under both anoxic and oxic conditions. The subsequent mobility of As, U and Mo was reduced *via* sorption to underlying sediments; however, potential exists for their transport in the groundwater flow system.

ACKNOWLEDGEMENTS

I would like to thank my supervisor, Matthew Lindsay for his ongoing support, insight, and feedback: these have been an integral part to this thesis. Thank-you to my advisory committee members for the help and advice you have provided throughout this process.

I would also like to acknowledge Canadian Nuclear Laboratories for working alongside me in the field and providing me with valuable information about my study site. Thank-you to the Sylvia Fedoruk Centre and the Global Institute for Water Security for financial support.

I would also like to thank the members of the Lindsay research group for your assistance with my laboratory work. Jake Nesbitt, Kaixian Qin, Mattea Cowell, and Colton Vessey thank-you for all of your help in the lab.

Lastly, thank you to my family, my in-laws, my friends, and my husband who have listened to my many struggles and encouraged me to keep moving forward.

TABLE OF CONTENTS

LIST OF FIGURES

LIST OF TABLES

LIST OF ABBREVIATIONS

ACS	American Chemical Society
AECL	Atomic Energy of Canada Limited
CMCF-BM	Canadian Macromolecular Crystallography Facility – Bending Magnet
CNL	Canadian Nuclear Laboratories
EDTA	Ethylenediaminetetraacetic acid
GIWS	Global Institute for Water Security
HXMA	Hard X-ray micro-analysis
IC	Ion chromatography
ICP-MS	Inductively coupled plasma - mass spectroscopy
ICP-OES	Inductively coupled plasma - optical emission spectroscopy
SFCCNI	Sylvia Fedoruk Canadian Centre for Nuclear Innovation
WMAF	Waste Management Area F
WHO	World Health Organization
XANES	X-ray adsorption near edge spectroscopy
XRD	X-ray diffraction

CHAPTER 1. INTRODUCTION

Low-level radioactive waste produced during processing of uranium (U) ores often contains elevated concentrations of potentially hazardous elements including U and arsenic (As). Associated elements including molybdenum (Mo) may also occur at elevated concentrations. Mobilization of these metalloids during infiltration or water table fluctuations may negatively influence groundwater quality. Uranium, As and Mo have potential to become mobile under changing geochemical conditions including the pH and Eh, which influence aqueous speciation, sorption-desorption reactions, and mineral solubility. These elements exhibit dissimilar geochemical behavior, which complicates long-term predictions of water quality in soils, sediments and aquifers. Nevertheless, a comprehensive understanding of processes and conditions controlling the release, transport and attenuation is essential for effective management of these wastes.

Field and laboratory research was conducted to examine controls on U, As and Mo mobility in a low-level radioactive waste deposit. This research was focused on contaminated soils overlying a shallow unconfined aquifer at Waste Management Area F (WMAF) at Chalk River Laboratories in Ontario, Canada. This geochemical study was performed as part of a larger study to constrain current hydrogeochemical conditions and to identify potential strategies for future management of this site. The research was conducted in partnership with Canadian Nuclear Laboratories (CNL), the Global Institute for Water Security (GIWS) at the University of Saskatchewan, and the Sylvia Fedoruk Canadian Centre for Nuclear Innovation (SFCCNI).

1.1. Study Site

Waste Management Area F (WMAF) is a low-level radioactive waste storage area located at Chalk River Laboratories in eastern Ontario, Canada (Figure 1). The waste is composed soil that is contaminated by a combination of slag from niobium refining, uranium refining waste, and radium dial paint residue. The waste was transported to the area from three locations in Ontario: Port Hope, Ottawa, and Mono Mills. Waste Management Area F is a cleared area surrounded by a forested landscape, with vehicle access from the north side. The western and southern ridges of the area are the face of a sand dune created by wind and decline of river levels

following glacial retreat from the area. Between 1976 and 1980 approximately 120,000 tonnes of contaminated soil waste were delivered to WMAF by truck.

The waste ranges from six to nine meters thick the thinnest being on the north side of the area and the thickest on the southwest, shown in the depth profile (Appendix 1 Figure A-1). Above the waste a clayey silt cover was constructed with a sand vegetation mixture on the surface, this cover is approximately two meters thick. The cover was constructed on top of the waste to minimize infiltration and limit potential for downward migration of U, As and other contaminants through the vadose zone. Underlying the waste is homogeneous fine grain sand that is coated with varying concentrations of iron oxides most commonly goethite and ferrihydrite.

The principal environmental concern of this site is As, U, and Mo leaching from the waste into the groundwater system due to failure of the cover overlying the waste. The general groundwater flow direction is toward the southwest of WMAF down a steep bedrock dip in the westward direction to a wetland referred to as “bulk storage swamp.” Waters from the bulk storage swamp eventually migrate to two lakes: Maskinonge Lake and Toussaint Lake (Appendix 1 Figure A-2). Wells were previously installed along the groundwater flow path to monitor potential contaminant transport in the saturated zone. There are two series of wells installed at WMAF: the GL series, and the LPH series (Appendix1 Figure A-3). Pore-water samples are taken from the wells for contaminant concentration determination. Testing is performed regularly to monitor groundwater flow and quality in the area.

Canadian Nuclear Laboratories (formerly Atomic Energy Canada Limited) conducted detailed investigations of contaminant transport and attenuation at WMAF in 1983 and 1993. Elevated dissolved As concentrations were observed in the vadose zone; however, these concentrations were generally consistent between the two studies and exhibited little change between the two studies. In the 1983 report it was determined that the cover had been largely ineffective, during the winter months the clayey silt had formed fractures which were then filled in with the permeable sand located above the silt layer allowing infiltration and preventing any swelling of the clay to repair the fractures. Consequently, it was determined that iron oxide coated sand underlying the waste was likely contributing to attenuation of the As leached from the waste. The report states that the As(V) is likely immediately sorbed to the sand underlying the waste and the As(III) is sorbed in deeper sand due to the oxidizing properties of the

permeable sands below the waste, or the reduced As species are oxidized to As(V) and then sorbed. In this 1983 report it was estimated that it would take between 10 and 100 years to exceed water quality guidelines in the pore waters beneath the underlying sands. In 1993 wells were drilled and sample obtained to perform spectroscopy, and fluorescence studies on and determine if immediate remediation action was required. It was determined that the As levels had not changed significantly between 1983 and 1993 but the dissolved and sorbed As was still present and the sorptive capacities or the sands would be reached in a few hundred years.

The 1993 report was the first study that U species were looked at and it was determined that there should be enough capacity for high levels of U to sorb to the underlying sands. There were however, small quantities of U found at the water table. The recommendation was made that remedial action should eventually be taken, but was not required immediately. It was suggested that the changes in the contaminant levels and site conditions be monitored to determine when action was required. Following these two studies annual monitoring has been carried out by AECL. Since the 1983 and 1993 studies, no detailed geochemical investigation has been performed.

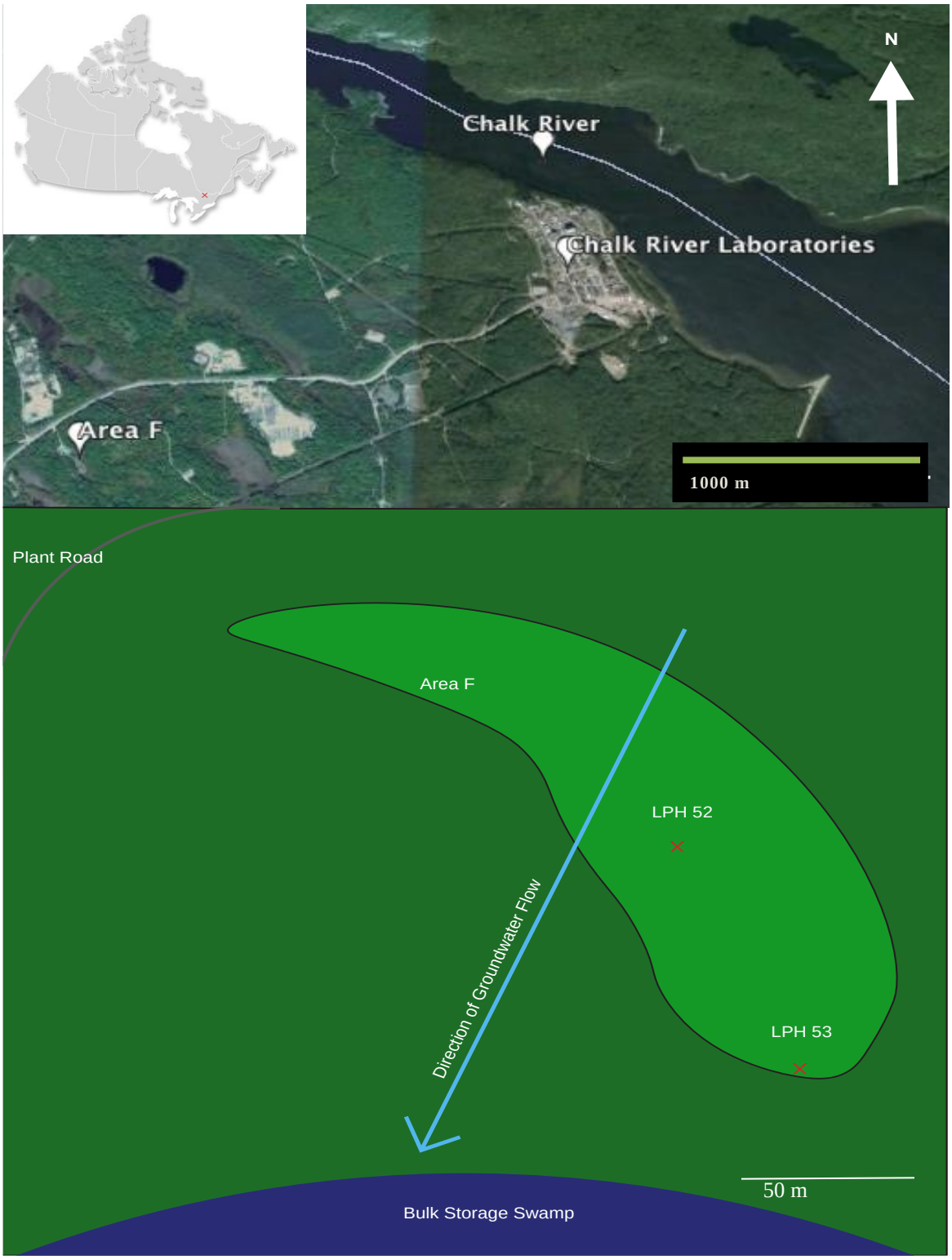

Figure 1.1. Schematic plan view images of Waste Management Area F. Showing marked drilling sites, and groundwater flow path. (Satellite Image Source: Google, DigitalGlobe, June 22, 2016).

1.2. Arsenic geochemistry

Arsenic is a period 15 metalloid that can occur in −3, 0, +3, or +5 oxidations states (Smedley and Kinniburgh, 2002); however, As(III) and As(V) are typically the most prevalent in the environment (Jones, 2007). Sulfide minerals including As-bearing pyrite [FeS_2] and arsenopyrite [FeAsS] are important geological As sources (Smedley and Kinniburgh, 2002). The natural weathering of sulfide minerals can release As to groundwater systems. Anthropogenic As sources include industrial waste, pesticides, herbicides, and wood preservatives (Smedley and Kinniburgh, 2002). Sorption onto metal oxides and hydroxides is a principal control on As mobility in soils, sediments, and aquifers (Deschamps et al. 2003); however, aqueous As speciation strongly effects the efficacy of this control on As mobility. Redox and aqueous complexation reactions strongly influence As speciation in groundwater systems. These reactions control the potential for sorption-desorption and precipitation-dissolution reactions that impact As mobility.

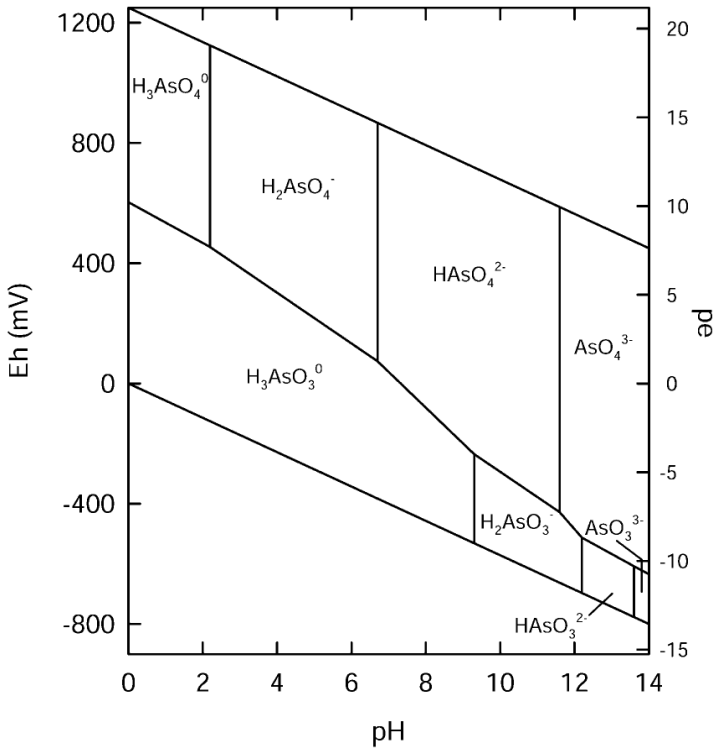

Figure 1.2. Pourbaix (pe-pH) diagram for As in the As-O2-H2O system at standard temperature and pressure. Based on results from studies of samples with 0.71-98 ppb As. (Reprinted with permission from Smedley and Kinniburgh. Copyright 2002 Elsevier).

Redox reactions that change the oxidation state between As(III) and As(V) can strongly influence As mobility. Arsenic(III) is generally more mobile than As(V) in groundwater systems due to differences in sorption behavior of associated aqueous species. Both As(III) and As(V) species form bidentate, inner sphere complexes with Fe(III) (hydr)oxide surfaces, which commonly exhibit net positive charge under acidic pH conditions (Parks, 1965). Dissolved As(V) occurs as oxyanions (i.e., $H_2AsO_4^-$, $HAsO_4^{2-}$) at pH values typical of groundwater systems (i.e., 5.5 to 8.5), whereas the neutrally-charged $H_3AsO_3^0$ is the dominant As(III) species at pH < 9. Consequently, As sorption is sensitive to changing redox conditions with enhanced mobility generally associated with As(V) reduction to As(III) (Kinniburgh and Smedley, 2002). The oxidation of As(III) to As(V) is less problematic, and can lead to an overall reduction in As mobility.

Parsons et al. (2013) studied what the outcome of oscillating redox conditions would be with regard to the mobility of Arsenic in natural soils. This phenomenon is commonly seen in areas where water table fluctuation is drastic between seasons. They performed a flooding experiment to determine the changes that may be occurring during a redox oscillation cycle and found that the Eh changed from oxic to anoxic to a great enough extent that it surpassed the $HAsO_4^{2-}/H_3AsO_3$ threshold and mobility would then become likely. The main mechanism that was found to control the mobility of As species in the redox cycling was reduction of poorly crystalline Fe-minerals. This suggests that the Fe-minerals present at the site, and the probability or extent of redox oscillation in the aquifer will greater limit or increase the mobility of As species.

Several minerals may control As mobility in groundwater systems. The most common minerals are Fe (hydr)oxides, Mn oxides, Fe sulfides (Smedley and Kinniburgh, 2002; Xie et al. 2014). Dixit and Hering (2003) found that As(V) sorption to Fe(III) (hydr)oxide minerals decreases with increasing pH (Figure 2). Although As(III) sorption may occur over a wide pH range, maximum As sorption tends to be lower than for As(V) (Dixit and Hering, 2003). These authors also observed that As(III) desorption occurred more quickly than for As(V). Jakobsen et al. (2006) found that As was more strongly bound to highly structured Fe(III) (hydr)oxide minerals compared to poorly amorphous precipitates.

Microbial reduction can also lessen the sequestration of As species in groundwater systems, by reducing As(V) to more mobile As(III) (Smedley, 2008). Microbial reduction of

Fe(III) (hydr)oxides can also mobilize As(III) species by reducing the mineral surface area available for sorption (Muehe et al., 2013). Kocar et al. (2006) observed preferential release of As(III) compared to As(V) from ferrihydrite-coated sand in laboratory column experiments. Xie et al. (2014) found that high As concentrations in groundwater in the Datong Basin in China generally corresponded to elevated dissolved Fe and Mn concentrations. When soils become flooded microbial consumption of O_2 can lead to the development of anoxic conditions (Burton 2014). These observations demonstrate that microbial reduction of Fe and Mn (hydr)oxides and/or As(V) can enhance As mobility in groundwater.

Burton et al. (2014) performed a series of soil/water experiments to determine the effect of microbial reduction of sulfate and its effects on the mobility and speciation of As in the soil. XANES spectroscopy showed that initially the As in the soil was in its oxidized As(V) form. After the soil was flooded XANES was performed again and it was found that a large portion of the As(V) was reduced to As(III) in the biotic experimental conditions, but not the abiotic conditions. This study also found that the reduction of As(V) happened alongside the reduction of the Fe-minerals that were present in the soil leading to desorption. This studies illustrates that following flooding of natural soil the release of As into groundwater is likely.

Precipitation of sulfide minerals especially pyrite may also contribute to As attenuation under sulfate reducing conditions (Kirk et al., 2004, 2010; Lowers et al., 2007; Savage et al., 2000; Farquhar et al., 2002). Arsenic exhibits similar chemical properties to S and, therefore, may replace or substitute for S in sulfide-mineral lattices (Smedley and Kinniburgh, 2002). This process can occur in conjunction with reductive dissolution of Fe(III) (hydr)oxides, with As released from Fe(III) (hydr)oxides subsequently incorporated into Fe sulfides (Lowers et al. 2007). Transformation of Fe(III) (hydr)oxides in the presence of dissolved sulfide species may also promote formation of magnetite, which has also been shown to promote As attenuation (Kocar et al., 2010). However, subsequent oxidative weathering of these sulfide minerals could potentially release attenuated As into the groundwater system (Langner et al. 2013).

Competition for sorption sites can also be controlled by the other species present in groundwater. The main competing ions are sulfate (SO_4^{2-}), phosphate (PO_4^{3-}), and carbonate (HCO_3^-). Dixit and Hering (2003) found that the first ion present, either PO_4^{3-} or As species, was more extensively sorbed. This finding means that the order these ions are introduced to a groundwater system may influence As attenuation via sorption. Because As and S exhibit similar

chemical properties, they are commonly found together in nature, which often results in sulfate competing with As for binding sites, producing higher levels of S and As species in groundwater systems. Phosphate is also a common competitor with both As(V) and As(III) for sorption sites; however, under strongly reducing conditions phosphate binds more weakly than As(III) (Smedley and Kinniburgh, 2002). Carbonate ions, which commonly occur at elevated concentrations in groundwater systems, can compete for sorption sites with both As(V) and As(III) (Appelo et al., 2002). Under reducing conditions, As(III) is present and carbonate can preferentially occupy available binding sites, thereby enhancing As(III) mobility.

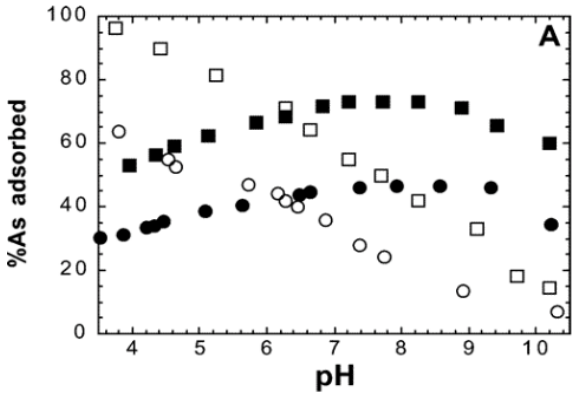

Figure 1.3. Sorption of As(V) (open symbols) and As(III) (closed symbols) onto amorphous iron oxide in equilibrium with initial dissolved As concentrations of 100 μg L^{-1} (circles) and 50 μg L^{-1} (squares) (Reprinted with permission from Dixit and Hering. Copyright 2003 American Chemical Society. Dixit and Hering, 2003).

1.3. Uranium geochemistry

Uranium is a period 7 metal that occurs naturally in geologic materials. The most abundant U isotope is U-238; however, U-235 and U-234 can also occur naturally. Uranium is the heaviest element that occurs in nature and is one of the most radioactive metals (Mkandawire, 2013). Uranium can be found in aqueous environments with oxidation states ranging from (III) to (VI); however, U(VI) is the most common and stable oxidation in groundwater systems (Mkandawire, 2013). Typical groundwater U concentrations are in the low parts per billion range (Alam and Cheng, 2014), however, both anthropogenic and natural contamination exists. Uranium contamination caused by weathering of naturally occurring deposits have been found, in the

United States, with contaminant levels of 10-700 µg L^{-1}, (Orloff et al., 2004 and Longtin 1998). Understanding the controls on U mobility in groundwater systems is important because exposure can cause serious health issues that include cancer and liver damage. Internal effects of U ingested through food, water, or air may result in internal irradiation or chemical toxicity, (Thomas Jefferson National Accelerator Facility - Office of Science Education, 2014). Similar to As, U mobility in groundwater systems is strongly controlled by redox processes, which influence aqueous complexation, sorption-desorption, and mineral dissolution-precipitation reactions. Numerous field and laboratory studies have been conducted to evaluate the conditions and processes controlling U mobility in the environment (e.g., Giblin et al., 1981; Ewing et al. 1992; Nriagu et al. 2012; Alam and Cheng, 2014). Although abundant information on geochemical processes controlling U mobility in groundwater has been reported, studies continue to find new and useful information (e.g., Campbell et al., 2012; Zachara et al. 2013; Mkandawire, 2013)

Redox processes have a substantial influence on U speciation in groundwater systems. The oxidation state of the U present in soil, sediment or aquifers impacts aqueous complexation and, therefore, U mobility. Uranium(VI) is the dominant oxidation state in groundwater systems (Fein et al. 2013) because of rapid U(III) oxidation in the presence of oxygen and limited solubility of the U(IV) phase uraninite [UO_2]. Uranium(VI) is highly mobile in groundwater because it forms soluble aqueous complexes over a wide pH range (Mkwandawire, 2013). Therefore, U mobility is generally enhanced in oxidized environments where U(VI) dominates (Edmunds et al. 1996). At pH less than 5, the dominant U(VI) species is $U(OH)_2^{2+}$, whereas $U(OH)_4$ generally dominates at higher pH.

Reduction of U(VI) to U(IV) can promote uraninite [UO_2] precipitation, which is an important control on dissolved U concentrations in anoxic groundwater systems (Finch et al 1992). However, reduction of U(VI) to U(IV) may be inhibited by the presence of aqueous complexes (Fein et al, 2013). Uranium(VI) commonly forms aqueous complexes with carbonate, sulfate and nitrate in groundwater systems (Banning et al. 2013). These complexes may be thermodynamically stabile in groundwater systems where Ca is present. Reduction to the less soluble U(IV) can greatly decrease the likelihood of high dissolved U concentrations occurring in groundwater systems (Bopp et al. 2010).

Sorption also greatly affects the mobility of U species in groundwater systems. Sorption to Fe(III) (hydr)oxides, organic matter and clay minerals, which are common in groundwater systems, can limit U transport in groundwater (Fein et al. 2013). Fein and Powell (2013), found that adsorption increased steadily from pH 3 to 5, reached a plateau at near neutral pH, and decreased again from pH 8 to 9. Sorption is strongly affected by the presence of competing species such as Ca^{2+}, which promotes formation of aqueous U complexes including $Ca_2UO_2(CO_3)_3^0$ and $UO_2(CO_3)_3^{4-}$ and can decrease sorption by up to 20% (Dong et al. 2005). Barnett et al (2002) found that in the presence of dissolved carbonate species sorption decreased significantly, especially at above neutral pH, which is expected due to the readily formed uranyl-carbonate complexes. Bea et al. (2013) found that enhanced weathering of carbonate based minerals under acidic conditions was increased thus resulting in release of U species in to the groundwater. Bea et al. (2013) also found that the specific surface area of the mineral present can have a significant effect on the attenuation of U, because the more available sites there are for U to sorb to the greater control there is on its mobility. Uranium complexation with dissolved organic matter which can enhance mobility by decreasing potential for sorption to mineral surfaces. Under typical groundwater pH conditions (i.e., 5.5–8.5), complexation of U with organic compounds such as humic acids does not significantly affect the transportation of U when there is a substantial quantity of inorganic ligands present (Ranville, et al. 2007).

Qafoku et al. (2014) studied the effect of co-contaminant sorption to determine the main sinks for U species in natural soils and factors influencing sorption. Extractions, XANES, XRF, and ICP-MS were performed to determine the forms and quantities of contaminants present in the samples and controls on their mobility. It was determined that As is a major competitor for sorption sites especially when the sink present in the soil is Fe-minerals. It was also found in this study that U(IV) is stable against changing redox conditions including re-oxidation of a system from groundwater recharge.

Precipitation of U-bearing minerals can also strongly influence U mobility in groundwater. In addition to reductive uraninite precipitation, precipitation of U(IV) phosphates dominate at low pH whereas uranyl silicates dominate at high pH (above 10) (Zachara et al., 2013). Although precipitation of these phases may limit dissolved U concentrations, weathering and oxidative dissolution which readily releases mobile U(VI) species in to the groundwater system.

Several significant processes that are all closely related control the mobility of Uranium in groundwater systems. The redox properties of a system dictate which U species is dominant which in turn determines the complexation, precipitation, or sorption can happen. To immobilize uranium in a groundwater system reducing conditions are required to convert the highly mobile U(VI) to the less soluble U(IV) which often results in reductive precipitation and immobilization of U, (Alam and Cheng, 2014).

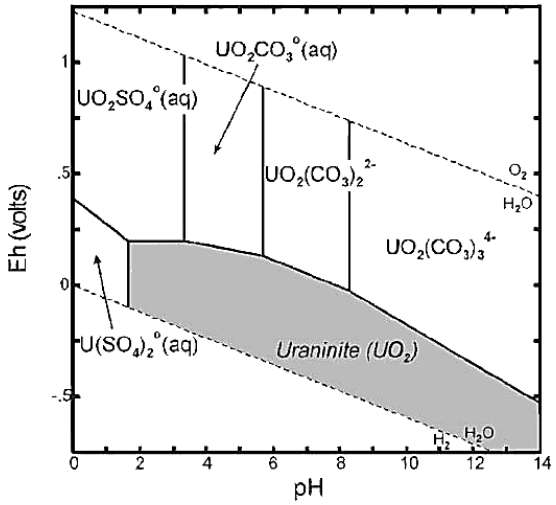

Figure 1.4. Eh/pH diagram for U species calculated at STP and a concentration of 10^{-7} mol L^{-1}. (after: Krupka and Searne, 2002).

1.4. Molybdenum geochemistry

Molybdenum is a period five transition metal. It is found as Mo(VI) in groundwater systems. Molybdenum has been found to be toxic to multicellular life if ingested at high quantities, although not much information is known about its effect on humans. The WHO standard for Mo intake is 70µg L^{-1}. This value was chosen based upon cases of increased molybdenum levels in multicellular organisms that caused enlarged liver, kidney failure, and gastrointestinal tract issues (WHO guidelines for drinking water quality, 2001). Although not many cases of increased molybdenum ingestion in humans have been studied, livestock has exhibited these effects which are common in areas where mining waste is stored. Molybdenum species are commonly found in sites where there is waste storage from mining and As and U are present. (Gustaffson 2003)

Molybdenite [MoS_2] is the most common Mo ore from which molybdenum is extracted to create steel alloys (Elwakeel, Atia, and Donia, 2009). Molybdenum is commonly found in high concentrations (>3μg L^{-1}) in groundwater systems due to its stability as an oxyanion and weak adsorption to minerals, (Bostick et al., 2003 and Smedley et al, 2002). Molybdenum oxyanion sorbs strongly to oxides from pH 2-4, however at pH values higher than 4 the sorption onto oxides decreases (Goldberg et al., 1996). Molybdenum can also be found naturally in the form of a thiomolybdate in anoxic environments. Molybdenum oxyanions can undergo a four step sulfidation reaction which conserves the Mo(VI) oxidation state, and results in the production of a tetrathiomolybdate species, (Erickson and Helz, 2000). Molybdenum transport and fate is strongly controlled by the pH conditions of a system, and is not drastically affected by the redox processes of the system.

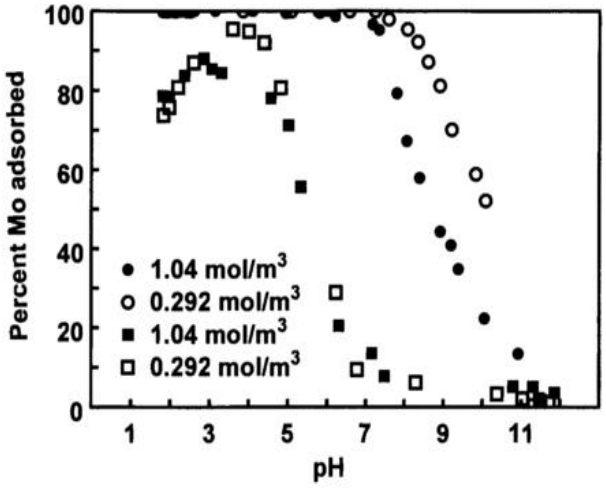

Figure 1.5. Molybdenum adsorption onto goethite (circles) and kaolinite (squares) as a function of pH from Goldberg and Forster (1998, use permitted without modification).

Molybdenum is prevalent in a +6 oxidation state at a pH >5 and an Eh > 0V (Anabar, 2004). Which is the reason for the decrease in its sorption properties at a pH of 4. Under these conditions the dominant oxyanion in solution is the tetrahedrally coordinated MoO_4^{2-}, however other oxyanion species may be present at various pH and Eh values. The oxyanion specie namely MoO_4^{2-} is not readily adsorbed to minerals and are highly mobile in geochemical systems with a circumneutral pH seen in groundwater where Fe oxides are a main control. (Anabar, 2004). Iron oxides have a negative surface charge in the pH range observed in groundwater systems (6-8) which lessens the affinity for sorption of the Mo oxyanion MoO_4^{2-} this affinity

increases with increasing acidity. (Xu et al. 2013; Heiz et al. 2011) If the pH value is less than 4 the MoO_4^{2-} may be protonated to form $MoO_3(H_2O)_3$ at high concentrations and low pH polymolybdates form (e.g., $Mo_7O_{24}^{5-}$ and $Mo_8O_{26}^{4-}$). (Xue et al., 2013)

Geng et al. (2013) used soil from a light bulb manufacturing company in Shanghai to do kinetic experiments to determine the equilibrium time between sorbed and aqueous Mo species in the soil when placed in solution and shaken. They also performed a batch experiment to determine the equilibrium between sorbed and aqueous Mo spcies when Fe-minerals were added into the natural soil system. The study found that the Mo species formed inner sphere bonds to goethite surfaces and that when the water was added to the system less Mo was able to sorb to the minerals due to the reactive hydroxyls in the system. The greatest sorption capacity for Mo species was found to be amorphous Fe-minerals. This give in sight to the sorption that may be observed in industrial soil management areas.

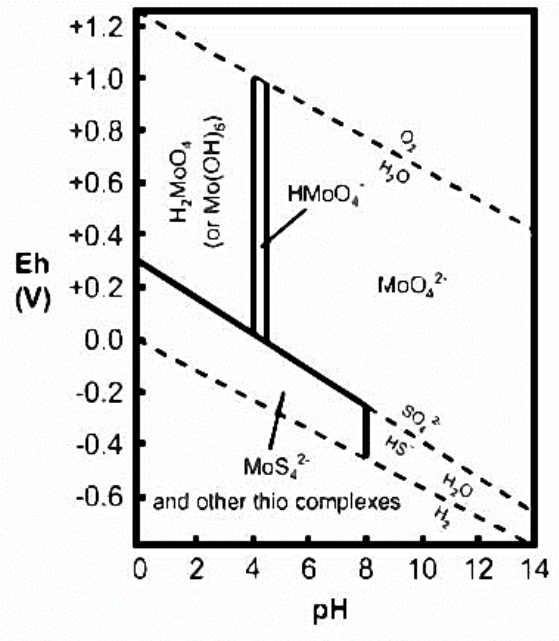

Figure 1.6. Eh/pH speciation diagram for Mo oxyanion species (after: Anabar, 2004).

1.5. Research hypothesis and objectives

Geochemical conditions, which may vary due to cover performance and water table fluctuations, will influence the mobility of As, U and Mo within contaminated soils at WMAF. The overall hypothesis for this research is that the contaminants at WMAF have not moved significantly through the waste into the underlying sand and will be stable for years to come;

however, there is potential for contaminant movement if conditions change. The specific objectives of this research project are to: (1) examine the occurrence and speciation of As, U, and Mo within WMAF; (2) determine under which conditions these contaminant elements may become mobile; (3) assess to what extent sorption onto underlying sand may limit transport.

This MSc research project involves a detailed investigation of the geochemical controls on dissolved As, U and Mo concentrations present at WMAF. This research was accomplished through integrations of bulk geochemical analysis, sequential geochemical extractions, synchrotron powder X-ray diffraction (SP-XRD), X-ray adsorption near edge structure (XANES) spectroscopy, leaching experiments, and batch sorption experiments. These experiments and measurements were conducted to provide new insight into the potential for As, U, and Mo leaching and transport under a range of geochemical conditions that could be encountered at WMAF. These contaminant elements exhibit enhanced mobility under disparate geochemical conditions: As mobility is typically greatest under anoxic conditions; U mobility is typically greatest under oxic conditions; and pH-dependent sorption is typically the dominant control on Mo mobility under both oxic and anoxic conditions. Overall, it was expected that the main controls on As, U and Mo mobility will be the oxidation state of the species, the pH of the system, and the presence of variably-charged mineral surfaces.

CHAPTER 2. METHODS

To predict the possible issues that will arise at WMAF in the future and test whether the findings of the previous studies were correct with regards to the leaching of As, U, and Mo species into the groundwater it was necessary to determine the current controls of the species. Sampling was done at the study site to prepare the appropriate samples for the various experiments that were performed to determine the geological characteristics of the site, and the conditions that are likely to control the As, U, and Mo species attenuation and release. Analysis was also performed to determine the oxidation states of the species present, the concentration of each species, and the distribution of the species within the depth profile of the site as well as the spatial distribution throughout the site.

The experiments that were performed were chosen based upon the literature and the results that were found in previous studies that have focused on the contaminants of interest. Column experiments were used to determine the quantity of each contaminant in the solid that was available to be released into the groundwater as well as the differences between anoxic and oxic environments because the study site has seasonal variations that are cause significant changes in the water table and could result in redox oscillations. The extraction experiment was performed to determine what the sorption sites for the contaminants are at WMAF. The batch experiment was performed to determine to what extent the sand underlying the waste at the study sites could sorb the contaminants present.

2.1. Sample collection

Sampling at WMAF was completed during the summer of 2014. A truck mounted drill rig was used to obtain samples of waste and underlying sand from the vadose zone at three locations throughout WMAF. Waste samples were collected at regular depth intervals from 0 to 10.45 m using a split spoon sampler. A full list of these samples with detailed descriptions is provided in Appendix 1 Table A-1. These samples were transferred to plastic bags, placed in a cooler on ice until they could be frozen, and shipped to the University of Saskatchewan. Sequential 0.76 m core samples of underlying sand were obtained over the 1.52 m interval immediately below the waste and then at 0.76 m spacing to a depth of 21.45 m. This interface is where the As, U and Mo accumulation was expected to be most abundant if leaching from the waste and subsequent attenuation via sorption had occurred. The cores were capped, placed on ice until they could be

frozen, and shipped to the University of Saskatchewan. Table 2.1 shows a summary of the collected samples that were used in the experiments performed.

Table 2.1. Sample descriptions and identification of use of samples in experiments performed.

Sample ID	Depth (m)	Description	XRD	XANES*	Digestion	Columns	SCE	Batches
LPH 52-6	1.8–2.1	Waste	X	As, U	X	X		
LPH 52-7	2.3–2.7	Waste	X		X		X	
LPH 52-8	3.1–3.4	Waste	X	As, Mo	X		X	
LPH 52-9	3.8–4.2	Waste	X	U, Mo	X	X		
LPH 52-11	5.3–5.8	Waste		U	X		X	X
LPH 52-12	6.1–6.4	Waste	X		X	X		
LPH 52-13	7.6–8.1	Fine sand			X		X	
LPH 52-14	8.4–9.1	Fine sand			X		X	
LPH 53-6	1.6–2.1	Waste			X	X		
LPH 53-8	3.1–3.5	Waste		U	X		X	X
LPH 53-9	3.8–4.3	Waste			X	X		
LPH 53-11	5.3–5.8	Waste		As	X		X	X
LPH 53-12	6.1–6.6	Waste			X	X		
LPH 53-13	6.9–7.0	Waste			X			
LPH 53-15	7.6–8.9	Waste			X		X	
LPH 53-16	9.1-9.6	Waste		As	X		X	X
LPH 53-18	9.9–10.5	Fine sand			X		X	

*only those that obtained useful data are noted.

2.2. Sample characterization

2.2.1 Whole-rock digestion

Whole rock digestion was done to determine the total quantities of species present in the samples that were retrieved from the waste area to understand the spatial variation and levels of the contaminants to compare to the levels obtained in other experiments performed. Subsamples were sent to ACME labs in Vancouver to be pulverized and characterized. Lithium borate fusion digestion with inductively coupled plasma mass spectroscopy (ICP-MS) was used to determine concentrations present in each sample. Samples were chosen based upon the mass of sample available for use in selective extractions and column experiments, see Table 2.1 for details on samples used. The samples were thawed, screened for radioactivity, sieved for removal of large particles, weighed (about 17 g of sample), and air dried in a fume hood. The samples were then reweighed to determine the water content, and sent to the lab for analysis.

2.2.2. As, U and Mo XANES

Bulk XANES spectroscopy was performed on beamline 06-ID-1 (HXMA) at the Canadian Light Source Synchrotron in Saskatoon, Saskatchewan, Canada. Following initial venting within a fume hood, the samples were transferred to an anaerobic chamber and dried within a vacuum desiccator. The dried samples were then powdered in an agate mortar and pestle and packed into 0.5 mm thick Teflon sample holders between two layers of 25.4 μm thick Kapton tape, and checked to make sure there were no pinholes present (i.e., to ensure no light was able to pass through the sample). Several samples were screened initially; however, due to concentrations below detection limits only those specified in Table 2.1 provided useful data. Spectra were obtained at the As K-edge (11867 eV), U L3-edge (17166 eV), and Mo K-edge (20000 eV) to examine the oxidation state and local coordination environment for these contaminant elements. The incident X-ray energy was selected using a dual Si(111) crystal monochrometer. The beam spot size was focused to 1 mm (vertical) by 3 mm (horizontal) on the samples. A minimum of three replicate spectra were obtained and averaged. Data reduction and analysis was performed using the ATHENA module of the DEMTER software package (Ravel and Newville, 2005).

2.2.3. X-ray diffraction

Synchrotron powder – X-ray diffraction (SP-XRD) was performed on beamline 08-B1-1 (CMCF-BM) at the Canadian Light Source in Saskatoon, Saskatchewan, Canada. Dried and powdered samples were packed into 0.8 mm diameter Kapton tubes. Diffraction patterns were collected over 90 seconds at 18 keV ($\lambda = 0.68879$) while the samples was continuously rotated with goniometer. The high-resolution back-illuminated charge-coupled device (CCD) area detector (Rayonix MX300-HE) was located 0.25 m behind the sample. Data processing was performed using GSAS-II software (Toby and Von Dreele, 2013). Detector geometry was calibrated using a LaB_6 standard. The capillary tube background was subtracted and resulting patterns were radially integrated using a 2θ resolution of 0.005°. Phase identification was performed using Match! (Version 3.1.0, Crystal Impact GbR, Germany) and the Crystallography Open Database (Gražulis et al., 2009).

2.3. Column leaching experiment

A column leaching experiment was performed to examine relationships between redox conditions and the mobility of As, U, and Mo. The column experiment was performed in two

parts; one set of six columns was placed on the bench top, and one set of six columns in the glove box, seen in Figure 2.1. Each week, 200 mL of deionized water was passed through the columns and the leachate was collected for inductively coupled plasma–mass spectroscopy (ICP-MS), inductively coupled plasma–optical emission spectroscopy (ICP-OES), and ion chromatography (IC). The columns were constructed of PVC pipe capped with nitex screens on the bottom to allow for water to pass through. They were then filled with 200 g of dry sample, and 250 g acid-washed sand mixed together to increase the permeability of the column to allow a faster flow, Table 2.2 describes the composition of each individual column. The sand and soil were mixed until a homogeneous sample was obtained and then packed into the tubes. Three soil samples were chosen from different depths in boreholes LPH52 and LPH53 including: (1) immediately below the waste/sand cover interface; (2) in the middle of the waste deposit; and (3) near the lower waste/underlying sand interface. Samples 1, 2, and 3 as referred to above were placed with the sand into the columns to simulate depth variability at the site. Once the columns were packed, they were placed in their respective environments and allowed to equilibrate for one week prior to the first leaching step. Deionized water wash flushed through both columns: for the bench top (oxic) experiment deionized water was used, for the glovebox (anoxic) experiment nitrogen was bubbled through deionized water for approximately 24 hours and then used. Each of the six columns were monitored weekly for twenty weeks with a transition between redox conditions – either oxic to anoxic or anoxic to oxic – occurring between week ten and eleven.

Table 2.2. Column Composition, redox conditions, and sample mass added.

Column ID	Redox Cycle	Mass Waste (g)	Mass Sand (g)
LPH 52-6B	Oxic–Anoxic	200.1	254.2
LPH 52-9B	Oxic–Anoxic	200.0	255.2
LPH 52-12B	Oxic–Anoxic	200.0	255.3
LPH 52-6A	Anoxic-Oxic	200.0	253.5
LPH 52-9A	Anoxic-Oxic	200.1	254.3
LPH 52-12A	Anoxic-Oxic	200.0	254.7
LPH 53-6B	Oxic–Anoxic	200.0	254.8
LPH 53-9B	Oxic–Anoxic	199.9	255.0
LPH 53-12B	Oxic–Anoxic	200.1	255.3
LPH 53-6A	Anoxic-Oxic	199.9	256.2
LPH 53-9A	Anoxic-Oxic	199.8	255.1
LPH 53-12A	Anoxic-Oxic	200.0	254.3

Figure 2.1. Photograph of the column experiment set up, six columns: 3 depths from each of 2 locations in WMAF.

To obtain water samples each week, the columns were weighed and the mass of the columns, prior to the addition of water, recorded. The water to be added was then weighed and the mass recorded. The weighed water was poured into the columns and allowed to pass through until all water droplets had stopped exiting the columns (approx. 30-45 min). The water obtained from the flow from each column was analyzed for pH, Eh, and alkalinity. Analysis of pH was

done with an Orion 8156 Ross Ultra probe that was calibrated to stock solutions with pH 4, 7, and 10; the probe was checked between each sample with the pH 7 stock solution to ensure proper readings were being taken. The pH values were recorded every minute until they were stable. The Eh was measured using a combination redox electrode (Orion 9678) with a Ag/AgCl fill solution (Orion 9000111) and calibrated with Zobell's solution (Zobell, 1946) and Light's solution (Light, 1972). Alkalinity was measured using 10 mL of the collected water, 2 to 3 drops of bromocresol green indicator, and either 1.6 N or 0.16 N H_2SO_4 until a pink color was achieved. Subsamples from the collected water were filtered and preserved with HNO_3 to be analyzed for metals by inductively coupled plasma mass spectroscopy (ICP-MS) and cations by inductively coupled plasma optical emission spectroscopy (ICP-OES). Subsamples were also collected and filtered with no preservation to be analyzed by an external lab for anions by ion chromatography (IC). After all collection pH, Eh, alkalinity measurements, and subsampling were completed the column was reweighed to determine its final mass after the water had passed through to determine the mass of water absorbed by the soil in the column. All subsamples were stored in HDPE bottles and refrigerated until shipped to external laboratories for analysis.

This procedure was followed every week for ten weeks. After the ten-week period, the columns were switched: the bench top columns were placed in the glove box, and the glove box columns were placed on the bench top, the columns were then allowed to equilibrate for one week. The sampling was then continued for an additional ten weeks following the same procedure under the new conditions.

2.4. Geochemical modelling

The geochemical speciation code PHREEQC was used to evaluate geochemical controls on the mobility of As, U and Mo (Parkhurst and Appelo, 1999). Thermodynamic equilibrium modelling of column leachate data provided insight into the aqueous speciation of these and other elements, and into mineral precipitation-dissolution reactions that may influence element mobility. The integrated Lawrence Livermore National Laboratory (LLNL) thermodynamic database was used in all simulations.

2.5. Sequential chemical extractions

A sequential chemical extraction (SCE) protocol was used to assess potential for mobilizing As, U, Mo, and other elements under varied geochemical conditions (Javed et al. 2013). Modifications were made to ensure the protocol was suitable and the method was going to effectively target the As, U, and Mo species present, and no final digestion was performed. The method was developed to avoid any issues with polyatomic interference of Cl-Ar for ^{75}As in mass spectroscopy. Five samples from different depths from LPH-52 and LPH-53 borehole locations were subjected to this sequential extraction protocol, fore description of samples refer to Table 3.1. One gram of the dry mass borehole soil was added to a 50 mL centrifuge tube and then 40 mL of each of the extraction solutions were added to the tube sequentially, following the procedure outlined in Table 3.3. After each solution was added, the samples were allowed to shake for the predetermined amount of time and centrifuged; the supernatant water samples were then collected, filtered, and acidified for analysis by ICP-MS.

Table 2.3. Sequential extraction protocol.

Fraction		**Reagent(s)**	**Preparation**	**Ratio (ml g^{-1})**	**Protocol**
ID	**Description**				
F1	Water soluble	Ultrapure water ($18^2 M\Omega cm$)	none	40:1	shake for 0.5 h @ room T; centrifuge @ 6000 x g for 40 min
F2	Strongly sorbed	1 M Na_2HPO_4	adjusted to pH 5.0 with 5N NaOH	40:1	shake for 16 h @ room T; centrifuge @ 6000 x g for 40 min; repeat for 24 h and pool supernatant
F3	Carbonate bound	1 M NaOAc	adjusted to pH 5.0 with HOAc	40:1	shake for 5 h @ room T; centrifuge @ 6000 x g for 40 min
F4	Co-precipitated with crystalline Fe, Mn, and Al (hydr)oxides	0.05 M $Ti(III)SO_4$ 0.05 M Na citrate 0.05 M EDTA 0.05 M $NaHCO_3$	adjusted to pH 7.0 using 5N NaOH	40:1	shake for 2 h @ room temperature; centrifuge @ 6000 x g for 40 min; repeat twice and pool supernatant
F5	Co-precipitated with amorphous Fe, Mn, and Al (hydr)oxides	1:2 vol. ratio of 30 % H_2O_2 to 0.2 M NH_4OAc	adjusted to pH 3.0 with 1 M oxalic acid	40:1	shake for 2 h in the dark @ room T; centrifuge @ 6000 x g for 40 min
F6	Acid soluble	16 N HNO_3	n/a	40:1	shake for 2 h @ room temperature; centrifuge @ 6000 x g for 40 min; repeat twice and pool supernatant

2.5.1. Preparation of extractant solutions

All chemicals used to make the solutions were purchased from Sigma-Aldrich. The first fraction was extracted using ultrapure (18.2 MΩ·cm) water; all subsequent extractant solutions were prepared using this water. For fraction two, 141.78 g of ACS grade (≥98%) Na_2HPO_4 were added to 1 L of milli-Q water, and stirred at a low heat until the solution was clear and colourless. This 1 M Na_2HPO_4 solution was then brought to pH 5 using a drop wise addition of 98% reagent grade NaOH. The fraction three solution was made by adding 82.03 g of 99% reagent plus grade NaOAc to 1 L of milli-Q water and then stirring until all solid was dissolved. This solution was then adjusted to pH 5 through the drop wise addition of ACS grade glacial HOAc before use. Fraction four was created using 99.9% trace metal basis $Ti(III)SO_4$, 99.5% BioUltra grade $HOC(COONa)_2(CH_2COONa)$, 99.995% trace metal basis EDTA, and 99.7% ACS grade $NaHCO_3$. A volume of 13.5 mL of $Ti(III)SO_4$, 14.71 g of $HOC(COONa)_2(CH_2COONa)$, 14.61 g of EDTA, and 4.2 g of $NaHCO_3$ were added to a flask and milli-Q water was added to 1 L, this mixture was then stirred until no solids were left and a transparent purple color was achieved. The solution was then adjusted to pH 7 through the drop wise addition of 5 N HNO_3. This fraction was shaken with tin foil around it to minimize photosensitivity of $Ti(III)SO_4$. For fraction five a 1:2 vol:vol ratio of 30% H_2O_2 and 1 M NH_4OAc was created using reagent grade ammonium acetate. A volume of 250 mL 30% H_2O_2 was added to 500 mL of 1 M NH_4OAc, which was made by adding 38.54 g of NH_4OAc to 500 mL of milli-Q water. This 1:2 solution was then adjusted to pH 2 through the addition of omni trace HNO_3. In the final fraction, 16 N trace metal grade HNO_3 was used.

2.6. Batch sorption experiment

A batch sorption experiment was performed to assess the sorption capacity of the sand for As, U, and Mo released from the waste. Leachates containing As, U and Mo were obtained in the same manner as described for the column experiments. The columns were composed of PVC pipe capped with nitex screens. They were then filled with 200 g of soil plus 250 g sand to increase the permeability of the column to allow a faster flow (for the composition of the samples used, refer to Table 2.1). The sand and soil were mixed until a homogeneous sample was obtained and then packed into the tubes. Half of the columns were left on the bench top and the others were put in the glovebox to model anoxic and oxic environments. Once the columns were packed they were allowed to equilibrate for one week prior to sampling. To obtain the

leachate, 200 mL of deionized (oxic) or nitrogen purged deionized (anoxic) water were flushed through the columns. A sand sample from the site was chosen based on its reddish color, which suggests there was a large concentration of iron present on the sand, and allowed for determination of the sorption capacity of the sand at WMAF. One gram (dry mass) of the sand was weighed out into a 50 mL centrifuge tube and 40 mL of the leachate obtained from the columns were added to each. The tubes were left to shake and the leachate was sampled at 1, 2, 4, 8, 16, 32, 64, and 128 hours. The original leachates as well as all samples obtained at the various sampling times were then sent to an external lab for trace metal analysis, pH, Eh, and alkalinity measurements were also taken at each sampling time.

2.7. Iron determination

To determine how much Fe was in the sand underlying the waste so that the potential sorption capacity could be found several sand samples from WMAF were sampled. The sand samples that were used in the batch experiment as well as sand samples underlying the waste taken at regular increments until 1m below the waste was reached were sent away to an external lab for trace metal analysis (ICP-MS). Six grams of sand was added into a 15mL centrifuge tube with 12 mL of HCl and shaken overnight. This sample was then diluted with 12 mL of deionized water, filtered, and taken to an external lab for trace metal analysis (ICP-MS).

CHAPTER 3. RESULTS

3.1. Solid-phase geochemistry

The waste composition was highly heterogeneous both chemically and physically. This study and the two previous studies (1983, 1993) revealed substantial spatial variation in contaminant element concentrations throughout the site. Depth- and borehole-dependent spatial trends in element concentrations were not apparent (Table 3.1, Figure 3.1). The bulk concentrations of As, U, and Mo in the WMAF waste ranged from 37 to 324 mg kg^{-1} (average 84.6 mg kg^{-1}), 9-95 (average 33.6 mg kg^{-1}), and 0.7-575 mg kg^{-1} (average 143 mg kg^{-1}) respectively. Other elements exhibiting elevated concentrations included: niobium (average of 507 mg kg^{-1} and a standard deviation of 1202.03 mg kg^{-1}), barium (average of 1134 mg kg^{-1} and standard deviation of 919 mg kg^{-1}), strontium (average of 335 mg kg^{-1} and a standard deviation of 49.5 mg kg^{-1}), cerium (average of 257 mg kg^{-1} and a standard deviation of 425 mg kg^{-1}), copper (average of 212 mg kg^{-1} and a standard deviation of 256 mg kg^{-1}), lead (average of 348 mg kg^{-1} and a standard deviation of 258 mg kg^{-1}), and zinc (average of 1100 mg kg^{-1} and a standard deviation of 2287 mg kg^{-1}). Total sulfur and carbon concentrations were 0.1 % (w/w) with a standard deviation of 0.03% (w/w) and 3.9 % (w/w) with a standard deviation of 1.9% (w/w), respectively.

Table 3.1. Summary of As, U and Mo concentrations from whole rock digestions.

Sample ID	Depth (m)	As (mg kg^{-1})	U (mg kg^{-1})	Mo (mg kg^{-1})
LPH 52-6	1.8–2.1	78.1	58.6	1.60
LPH 52-7	2.3–2.7	47.0	8.90	103
LPH 52-8	3.1–3.4	37.1	13.6	575
LPH 52-9	3.8–4.2	62.6	83.9	575
LPH 52-11	5.3–5.8	144	94.7	18.8
LPH 52-12	6.1–6.4	114	36.5	2.00
LPH 52-6	1.6–2.1	26.6	42.5	1.30
LPH 53-8	3.1–3.5	70.7	74.3	1.90
LPH 53-9	3.8–4.3	92.8	45.5	0.70
LPH 53-11	5.3–5.8	81.3	22.1	310
LPH 53-12	6.1–7.0	324	10.0	398
LPH 53-15	8.4–8.9	52.8	17.6	235
LPH 53-16	9.1–9.6	206	13.5	197
Average		**84.6**	**33.6**	**143**

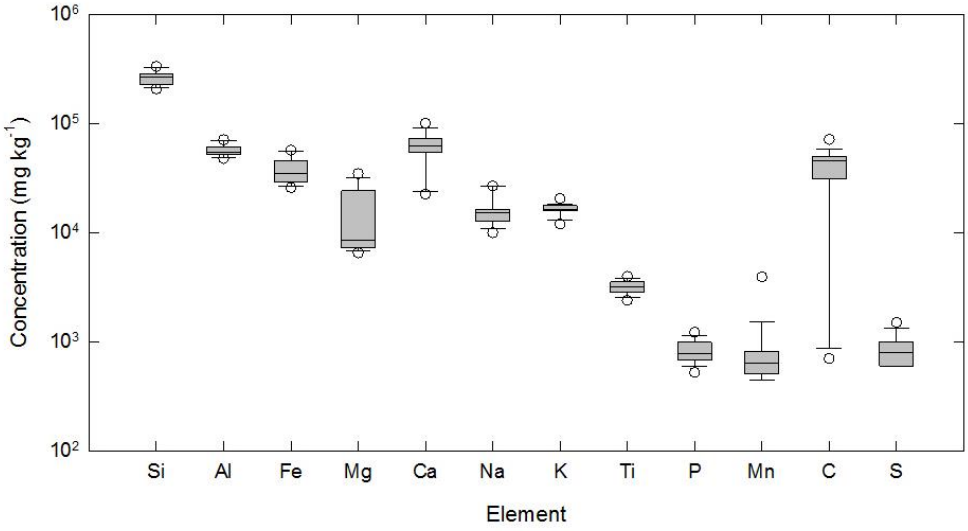

Figure 3.1. Major element concentrations from whole rock data. Median (line), 75th percentile (box), 95th percentile (whisker), outliers (circles).

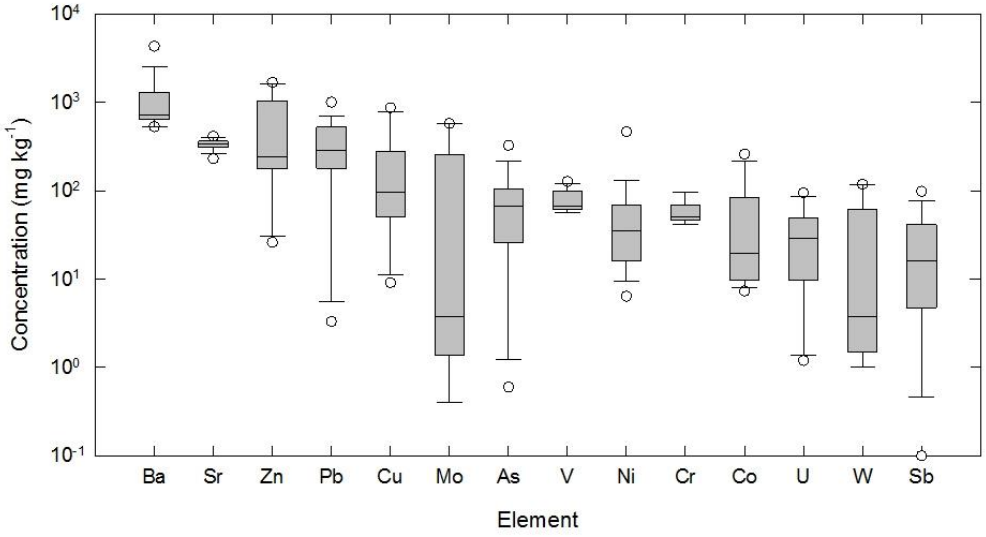

Figure 3.2. Minor element concentrations determined by fusion bulk digestion and ICP-MS. Median (line), 75th percentile (box), 95th percentile (whisker), outliers (circles).

3.2. Mineralogy

Several rock-forming minerals were present in the waste samples including quartz [SiO_2], orthoclase (potassium) feldspar [$KAlSi_3O_8$], calcite [$CaCO_3$], dolomite [$CaMg(CO_3)_2$], and anorthite [$CaAl_2Si_2O_8$]. Aluminum and iron(III) (oxy)hydroxide phases were also detected in select samples; however, these (oxy)hydroxides were likely minor phases within the waste deposit, shown in Figure 3.3 and Table 3.2. Because of the physical and chemical heterogeneity of WMAF, there were no specific trends in mineral distribution either with depth or location. Arsenic, uranium and molybdenum are likely to be incorporated into or sorbed onto the structures of calcite, dolomite, anorthite, iron oxides, and aluminum oxides, this phenomenon is supported by several studies. (Appelo et al. 2002; Ayoub et al. 2007; Dong et al. 2005; Golberg et al. 2002; Golberg et al. 2006)

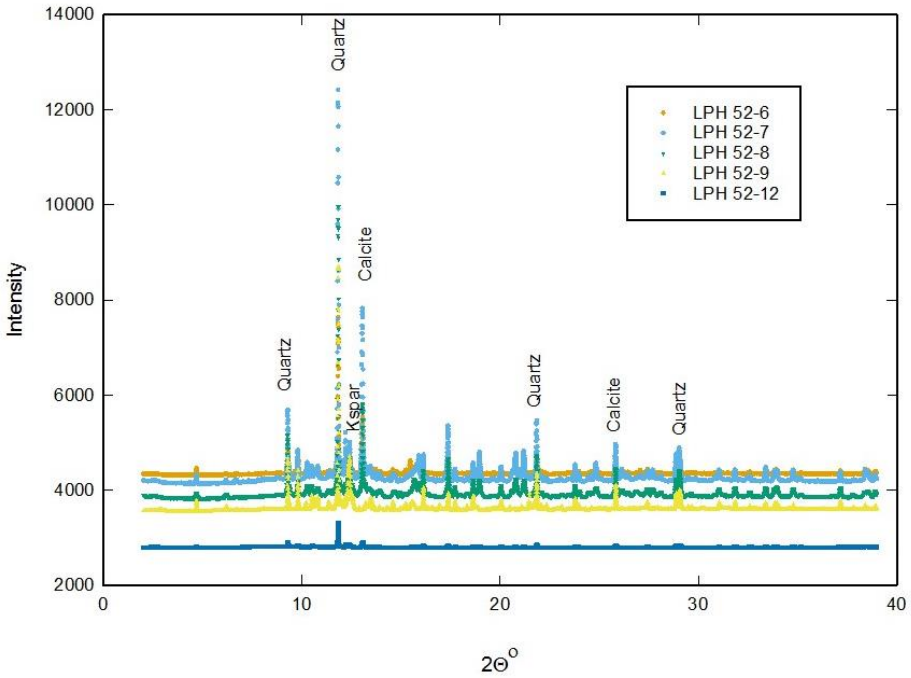

Figure 3.3. Results of SP-XRD analysis for samples from location LPH 52 annotated with diagnostic peaks for major mineral phases.

Table 3.2 XRD Results including depth, primary minerals, and other possible minerals present.

Sample ID	**Depth (m)**	**Primary phases**	**Other possible phases**
LPH 52-6	1.8–2.1	Quartz, calcite	Mo, As oxides
LPH 52-7	2.3–2.7	Quartz, K-spar, dolomite	Graphite, As oxides
LPH 52-8	3.1–3.4	Quartz, anorthite, dolomite, zinc	Ca, Mg, Al oxides/phases
LPH 52-9	3.8–4.2	Quartz, anorthite, dolomite, calcite	Mo, As, Mg oxides, La, Ce
LPH 52-11	5.3–5.8	Quartz, anorthite, calcite	Fe, Cu, Pb oxides/phases
LPH 52-12	6.1–6.4	Quartz, anorthite, calcite, Fe_3O_4	Fe_3O_4, Pb oxides, steel
LPH 52-13	7.6–8.1	Quartz, anorthite	Mo, La, As oxides
LPH 52-14	8.4–9.1	Quartz, anorthite	Mo, Ti oxides
LPH 53-6	1.6–2.1	Quartz, anorthite, calcite	Mo, As Oxides
LPH 53-8	3.1–3.5	Quartz, calcite	Ba, Mo, As, Cr oxides
LPH 53-9	3.8–4.3	Quartz, anorthite, calcite	Mo, As oxides; Al, Mg phases
LPH 53-11	5.3–5.8	Quartz, graphite, dolomite, calcite	Mo, As oxides; Ce, Fe sulfides
LPH 53-12	6.1–6.6	Quartz, dolomite, anorthite, calcite	La, Ce alloys
LPH 53-15	8.4–8.9	Quartz, dolomite	Graphite
LPH 53-16	9.1–9.6	Quartz, dolomite, anorthite, calcite	Fe, Cu sulfides; Ce, La alloys; Cu, Fe sulfides
LPH 53-18	9.9–10.4	Quartz, anorthite	Fe, Mo, As oxides

3.3. Solid-phase As, U and Mo speciation

X-ray absorption near edge structure spectra were obtained at the Canadian Light Source synchrotron to examine forms of As, U and Mo elements in WMAF (Figure 3.4). The As K-edge XANES spectra indicated that both As (V) and As (III) were present. The white line maxima generally corresponded to As (V) at approximately 11874.5 eV, whereas shoulders positioned at approximately 11870 eV was characteristic of As (III). The relative magnitude of the As(III) shoulder to the main As(V) edge varied among samples. Decreases in the relative size of the shoulder with depth at both of the borehole sites, LPH-52 and LPH-53, suggested that the relative proportion of solid-phase As(III) decreased with depth.

The U L_3-edge XANES spectra exhibited white line maxima between those observed for the U(IV) and U(VI) reference spectra. The white line maxima for the UO_2 and $UO_2(CO_3)$ spectra were positioned approximately 2 eV apart at 17175.5 eV and 17177.6 eV, respectively. The maxima for samples from LPH-52 and LPH-53 were consistently positioned within the range between these two reference materials. This observation suggests that both U(VI) and U(IV) species were present in the samples.

The Mo K-edge XANES spectra were more complex, but indicated that Mo(VI) was the dominant oxidation state. A pre-edge peak observed in both samples was positioned at 20005 eV (centroid) as observed in reference spectra for Na_2MoO_4 and MoO_4 sorbed to ferrihydrite (Mo(VI)-Fh). The observed decrease in the magnitude of this pre-edge peak in the samples relative to the reference spectra is likely indicative of a change in Mo(VI) coordination (Ressler et al., 2000).

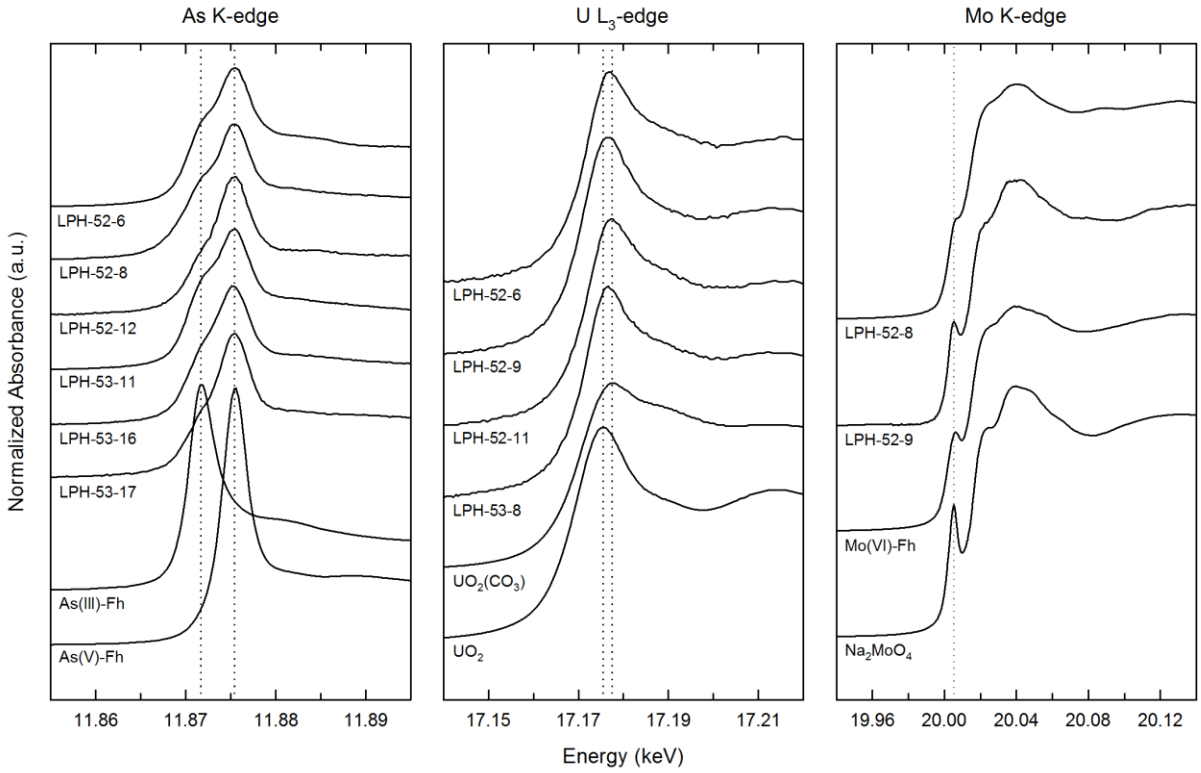

Figure 3.4. X-ray absorption near edge structure spectra collected at the As K-edge, U L_3-edge and Mo K-edge for samples and reference materials.

3.4. Column leachate chemistry

Leachate from the column experiments exhibited distinct trends in As, U and Mo mobility that were linked to both redox conditions, alkalinity and pH. The pH trend that was seen in the columns starting in the anoxic environment was a gradual decrease from week 1-10 and then when the columns were switched to the oxic environment a gradual increase was seen. The pH trend of the columns starting in the oxic environment was the opposite; there was a gradual increase in the first ten weeks followed by gradual decrease from week 10-20 when the columns were exposed to the anoxic environment. The pH value stays fairly close to the usual groundwater range in both sets of columns, (5.5-8.5). The pH trends and the specific values observed can be seen in Figure 3.5. The pH trend in both sets of columns can be attributed to the aqueous carbonate system and the carbonate complexes that can form in this system releasing H^+ ions, (Krupka and Searne, 2002). The Eh values of the leachates were as expected; the anoxic environments had more negative Eh values and the oxic showed values that were more positive. The Eh values slowly changed and became opposite after the switch from anoxic to oxic or oxic

to anoxic, these trends can be seen in Figure 3.5. The alkalinity of the columns was significantly higher in the anoxic environment than in the oxic environment regardless of the initial redox environment. These trends are indicative of release of As under anoxic conditions with potential for sorption and retention under oxic conditions and the release of U under oxic conditions with retention potential in anoxic conditions. The pH above 4 and Eh higher than 0V in the oxic conditions also creates the potential for release of Mo species into the leachate.

The leaching behaviors that were seen for As and U are consistent with what was expected based upon previous studies and can be seen in Figures 3.5 and 3.6, (Dixit and Hering 2003; Giblin et al., 1981; and Goldberg et al, 1996). Arsenic release was limited over 10 weeks under oxic conditions, but when columns were placed in anoxic conditions the mobility steadily increased over the second 10 weeks of the study. Effluent As concentrations were 3.13 mg L^{-1} for the initial 10 weeks for all columns under oxic conditions, but increased to to 5.34 mg L^{-1} following the transition to anoxic conditions. In the column setup for anoxic to oxic conditions, the ratio of release was 22.17 mg L^{-1}compared to 3.19 mg L^{-1}. In the column setup for anoxic to oxic conditions the ratio of release (the cumulative mass released per kg of dry soil) was 12.5 mg kg^{-1} compared to 0.07 mg kg^{-1}. In the column setup for oxic to anoxic conditions the ratio of release was 0.60 mgg^{-1} to 3.15 mg kg^{-1}. Uranium mobility generally exhibited the opposite behavior. Effluent U concentrations were 21.20 mg L^{-1} for the initial 10 weeks for all columns under oxic conditions, but decreased to 5.34 mg L^{-1} following the transition to anoxic conditions. In the column setup for anoxic to oxic conditions, the ratio of release was 3.34 mg kg^{-1}compared to 9.01 mg kg^{-1}. In the column setup for oxic to anoxic conditions the ratio of release was 6.30 mg kg^{-1} to 0.76 mg kg^{-1}. The column data confirmed that As leaching is greatest in anoxic conditions, while U leaching is greatest in oxic conditions regardless of the conditions the columns started in. These results are further supported by the PHREEQC modelling results. The model showed that within the pH conditions of the groundwater system (between 6-8) As(III) would be dominant in the anoxic environment and U(IV) would be dominant in solution. The dominant As(III) species was $HAsO_2$, and the dominant As(V) species was $HAsO_4^{2-}$. The dominant U(IV) species was $U(CO_3)_4^{4-}$. The results for the oxic conditions showed that the dominant species found would be As(V) and U(VI). The dominant As(V) species was found to be $HAsO_4^{2-}$ and the dominant As(III) was $HAsO_2$. The dominant U(VI) species was $UO_2(CO_3)_3^{4-}$ and the dominant U(IV) species was $U(OH)_4$.

Molybdenum leaching was not influenced by either the anoxic or oxic environments as expected, but was mobile throughout the entire experiment and was solely controlled by the pH of the system which was mimicked the values expected for a groundwater system, shown in Figures 3.5 and 3.6. Effluent Mo concentrations were 58.79 mg L^{-1} or the initial 10 weeks for all columns under oxic conditions, but decreased to 13.39 mg L^{-1} following the transition to anoxic conditions. In the column setup for anoxic to oxic conditions, the ratio of release was 44.83 mg L^{-1}compared to 13.86 mg L^{-1}. In the column setup for anoxic to oxic conditions the ratio of release was 22.9 mg kg^{-1} compared to 12.9 mg kg^{-1}. In the column setup for oxic to anoxic conditions, the ratio of release was 7.11 mg kg^{-1} to 2.53 mg kg^{-1}. This trend shows a steady decrease over the entire 20-week experiment until no Mo is available to be released and then a slow plateau is reached.

The behavior of Fe and Mn are important to acknowledge because U and As can sorb to Fe and Mn oxides which can potential act as a control on the mobility of the contaminants at WMAF. Both Fe and Mn were leached from the columns under anoxic conditions, shown in Figure 3.8. When the column started in anoxic conditions higher concentrations of Fe and Mn were observed, 11.6 mgL^{-1} and 1.51 mgL^{-1} respectively. In contrast the columns that were changed to anoxic conditions at ten weeks saw a maximum of 4.41 mgL^{-1} of Fe and 0.24 mgL^{-1} of Mn. Iron oxide and Mn oxide reduction is evident. The reduction of these species will result in soluble Fe(II) and Mn(II) phases resulting in the release of the sorbed contaminants.

The major ion chemistry showed no significant changes between anoxic and oxic conditions. In general, the concentration of the ions released was higher at the start of an anoxic or oxic experimental segment. Chloride concentrations were fairly low in all columns in all conditions with the greatest concentration being 7 mgL^{-1}. Nitrate concentrations were usually below 1 mgL^{-1}, and in one case up to 9 mgL^{-1}. Sulfate concentrations were between 20 and 90 mgL^{-1} regardless of the conditions. Calcium concentrations were observed between 15 and 60 mgL^{-1} in all conditions. Magnesium had concentrations below 15 mgL^{-1} in every condition studied. Sodium had a wide range of concentrations observed between 8 and 60 mgL^{-1} this was solely dependent on the sample, not the conditions. Potassium concentrations were low and were all below 8 mgL^{-1}.

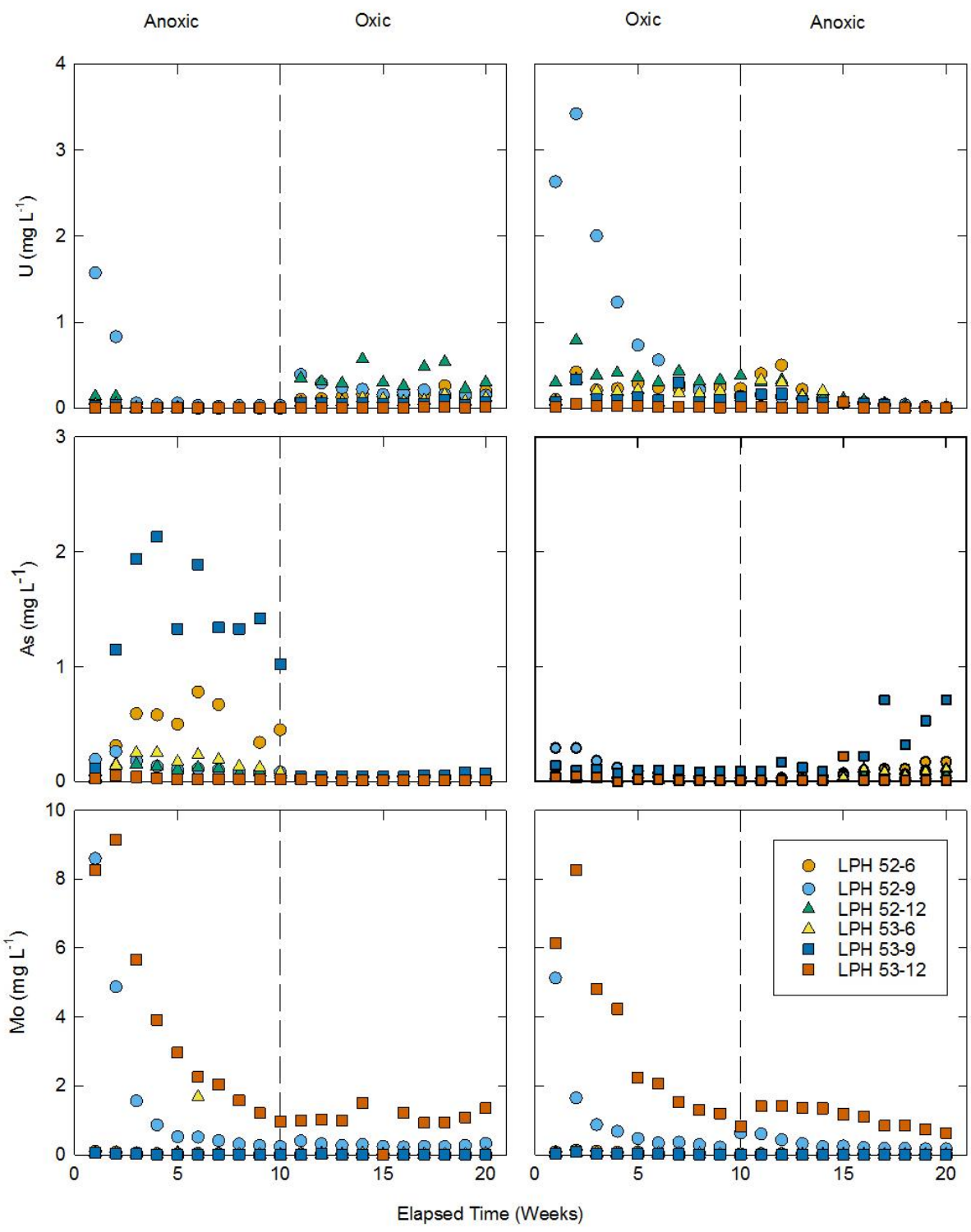

Figure 3.5. Effluent concentrations of As, U and Mo over time in column leaching experiments. Vertical dashed line indicates the transition in redox conditions.

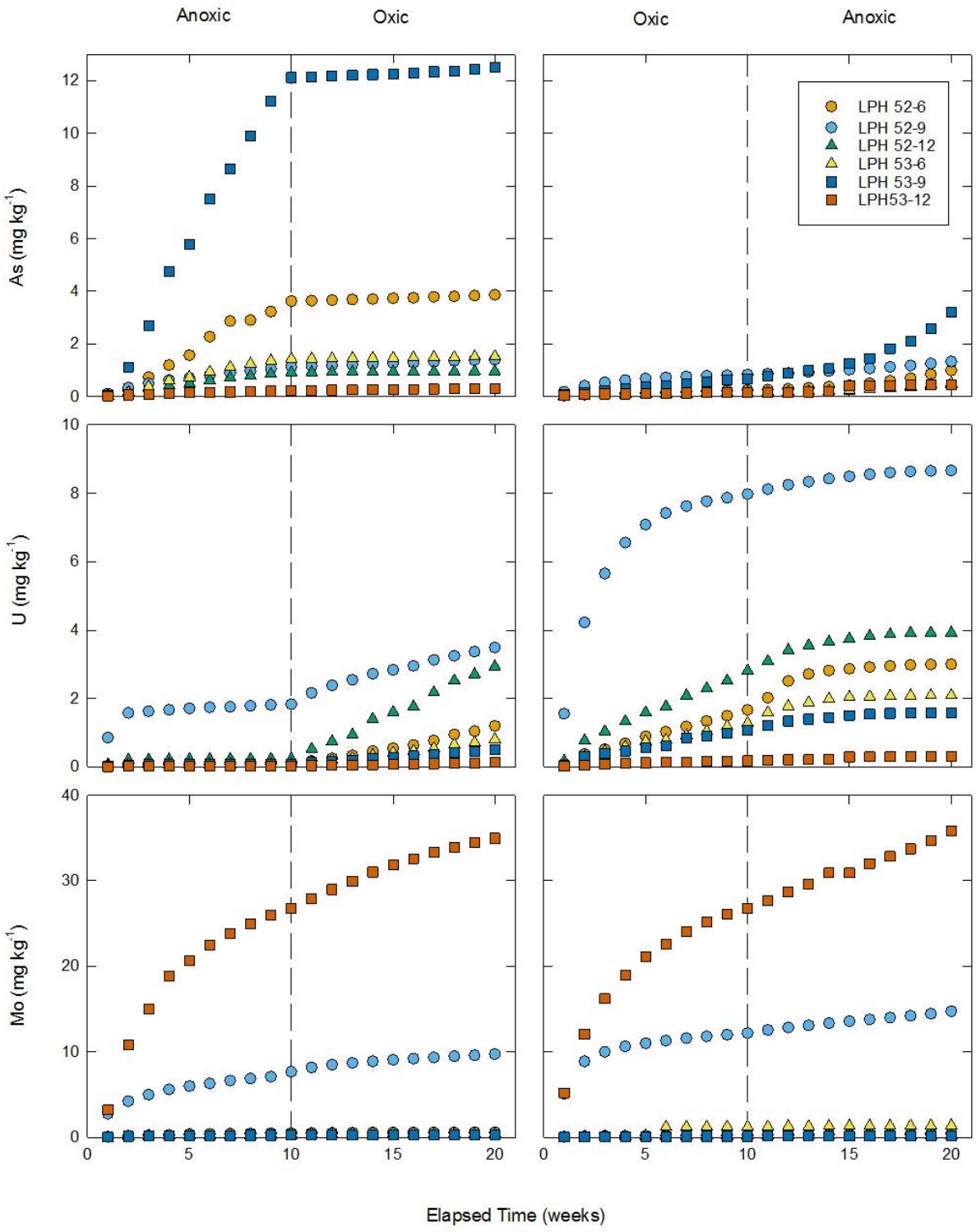

Figure 3.6. Cumulative mass release of As, U and Mo over time. Vertical dashed line denotes transition in redox conditions.

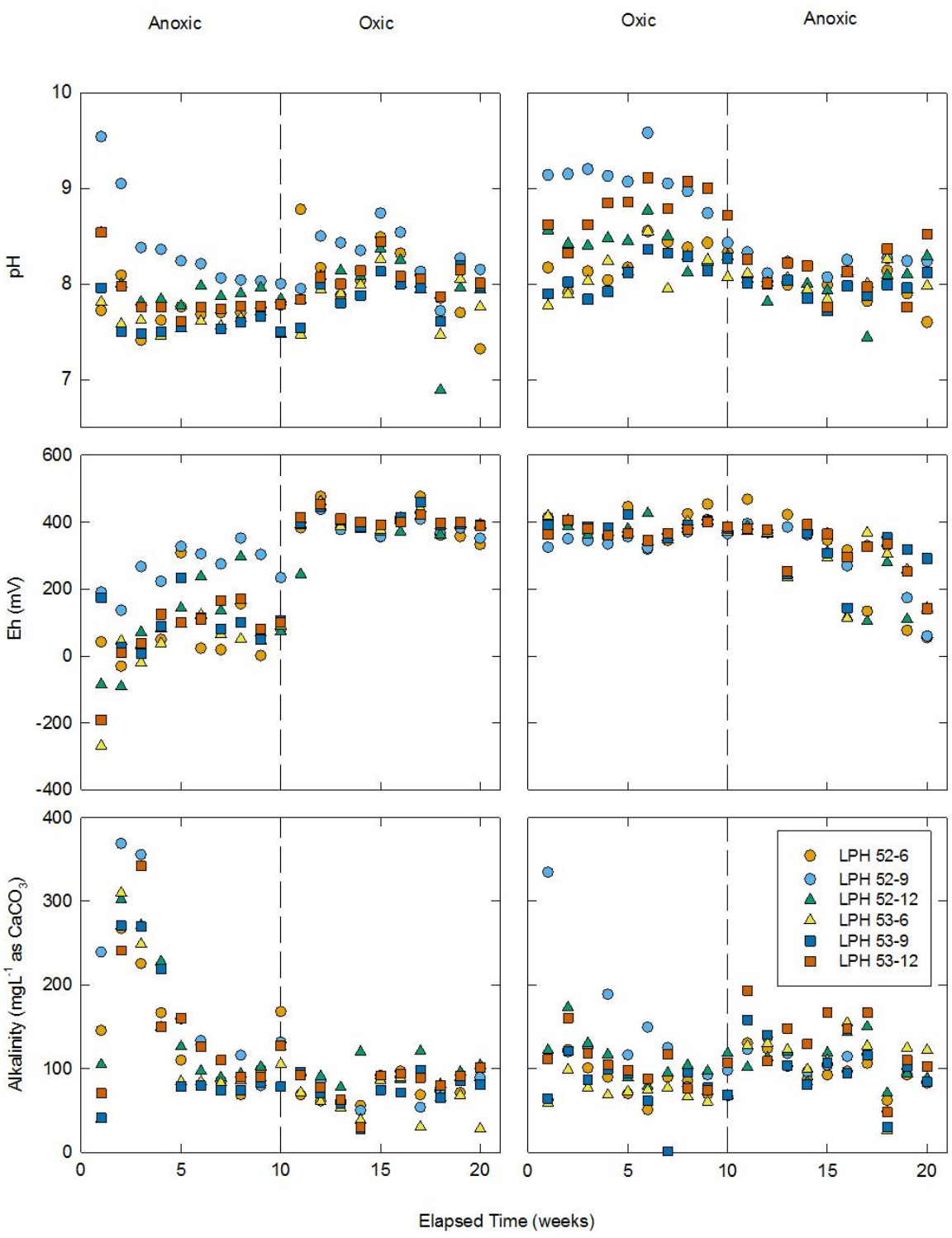

Figure 3.7. pH, Eh and Alkalinity concentrations over time in leachate. Vertical dashed line indicates transition in redox conditions.

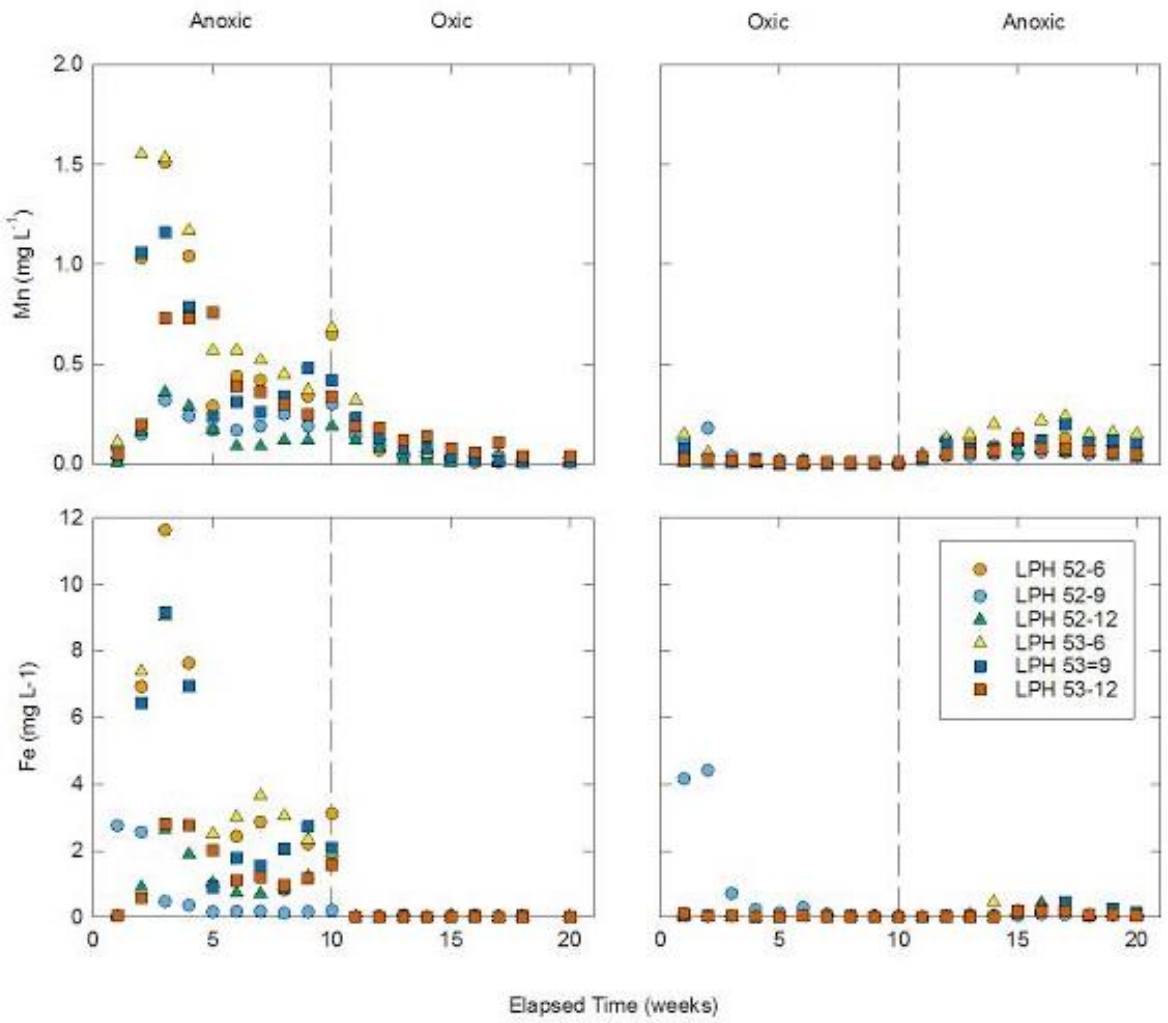

Figure 3.8. Iron and Manganese concentration over time in leachate. Vertical dashed line indicates transition in redox conditions

3.5. Sequential extractions

The sequential extractions were done for six fractions: F1 (water soluble), F2 (strongly sorbed), F3 (carbonate bound), F4 (co-precipitated with Fe, Mn, Al hydroxides), F5 (associated with organic matter), and F6 (acid soluble). Arsenic was largely extracted from the strongly sorbed (4.76 mg kg^{-1}), co-precipitated with Fe, Mn, and Al hydroxides (15.56 mg kg^{-1}), and acid soluble fractions (16.07 mg kg^{-1}). Uranium was found primarily in strongly sorbed (13.46 mg kg^{-1}), co-precipitated with Fe, Mn, and Al hydroxides (4.46 mg kg^{-1}), and in the acid soluble fraction (6.59 mg kg^{-1}). Molybdenum was removed from most of the fractions in significant proportions, however not much was removed from the co-precipitated with Fe, Mn,

and Al hydroxides, and acid soluble fractions, results can be seen in Figure 3.9. The maximum Fe that was removed was in F4 (442.44 mg L^{-1}) and the maximum Mn removed was in F5 (9.39 mg L^{-1}), these results support the hypothesis that reductive dissolution can be a mechanism of mobility for the three contaminants because as the Fe and Mn are reduced they will release the contaminants that are sorbed. Due to the heterogeneity of the samples, there were instances where extracted masses equated to greater than 100% of the total concentration of a given element.

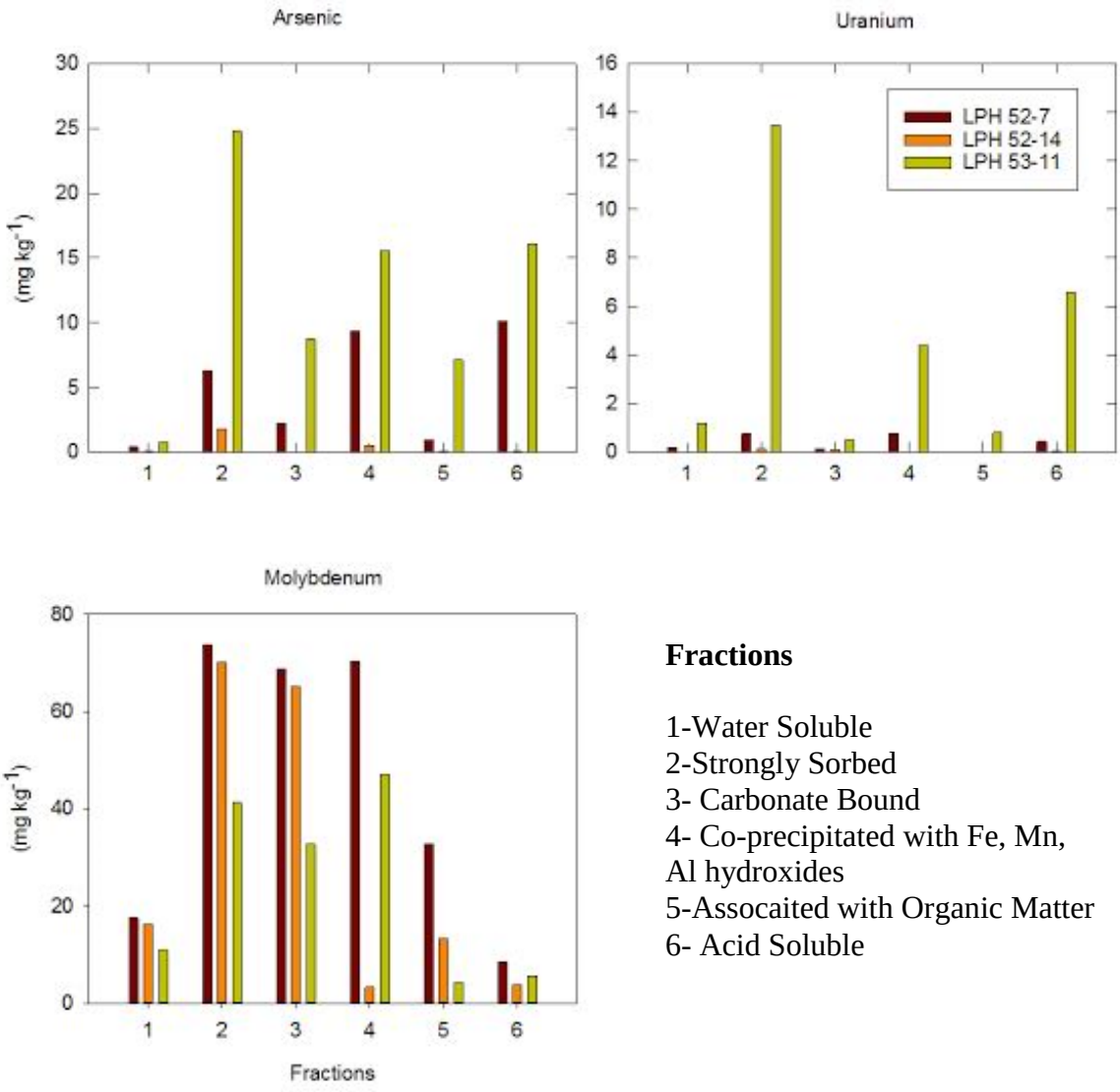

Figure 3.9. Sequential Extraction Data. Concentration of sorbed contaminants in each fraction.

3.6. Batch Experiments

The batch experiment was done to study the sorption behavior exhibited by the As, U, and Mo onto the underlying sands at WMAF, (Figure 3.10). In anoxic conditions the sand samples sorbed up to 35% of the As in the leachate, and 90% of the U in the leachate. In oxic conditions almost 100% of the U in the leachate from one sample and 60% from the other was sorbed. The As showed unexpected behavior in the oxic conditions, it had a negative sorption in one situation, and almost 100% in the other. Molybdenum also showed some negative sorption values in both oxic and anoxic situations. Under anoxic conditions, up to 5% of the molybdenum in the leachate was sorbed; however, under oxic conditions, Mo sorption was not observed. The negative values for sorption that were observed could be due to chemical changes in the solution over time (e.g. pH changes) and the initial presence of As, U, or Mo on the sand samples. The partition coefficients (K_d) values were calculated for As, and U experiments that followed the expected sorption isotherm curve, values can be seen in Table 3.3. The values were calculated using the following Freundlich model equation:

$$K_d = \left[\frac{\left(C_i / C_{eq}\right)}{C_{eq}}\right] \times \left(\frac{V}{m}\right)$$

Where: C_i = the initial concentration of the contaminant in the solution added to the sand

C_{eq} = the final concentration of the contaminant in the solution after sorption to the sand

V = the volume of solution added to the sand

m = the mass of the sand

Table 3.3 Calculated partition coefficients for batch experiments.

Sample	Contaminant	Partition coefficient (K_d)
LPH 52-11	As	0.0112
LPH 53-11	U	0.2918
LPH 53-16	U	0.5881

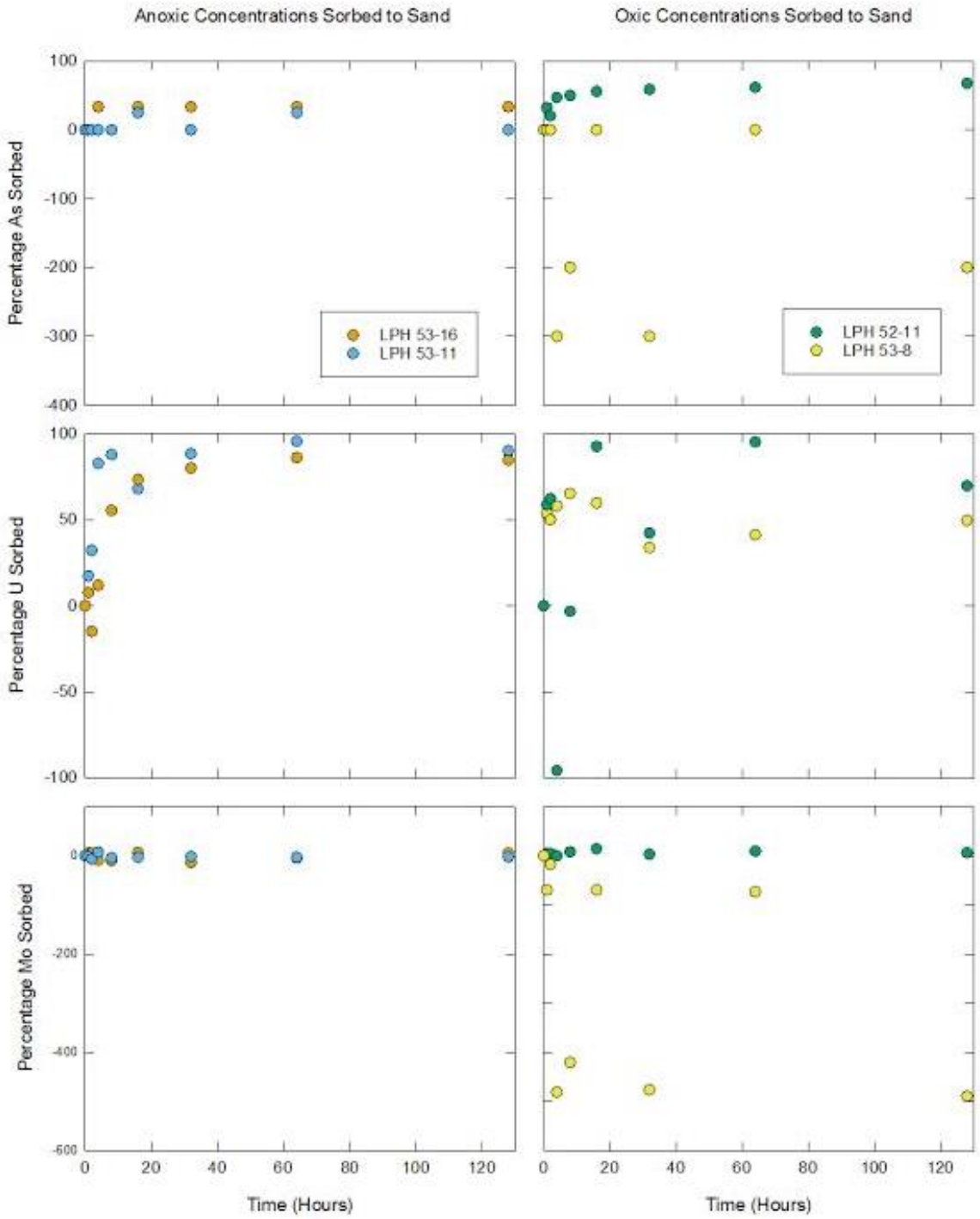

Figure 3.10. Batch Experiment Data. Percentage of sorbed contaminant over time.

CHAPTER 4. DISSCUSION

4.1. Arsenic

The XANES data showed that both As(V) and As(III) species were present in both of the locations that samples were obtained from at WMAF. This supports the hypothesis that both species are present at the site and that all situations and redox systems must be considered to determine the fate of the WMAF site. Arsenic species showed elevated leaching under anoxic conditions compared to oxic conditions. Similar results were observed when redox conditions were transitioned after 10 weeks of the experiment. This behavior can be attributed to the reductive dissolution of Fe(III) to Fe(II) alongside the reduction of As(V) to As(III) under anoxic conditions. This behavior also supports the finding that less As(III) species sorbed in the XANES experiment than As(V) due to the movement of As(III) through the system and the greater attenuation of As(V). This phenomenon has been seen several times before, and it has been concluded that although As(III) sorbs to the hydroxide surfaces over a larger pH range, however As(V) sorbs more strongly and to an overall greater extent (Dixit and Hering, 2003; Marin et al. 1993). It has also been observed that an increased withdrawal rate or flooding of soils subsequently increases the amount of As species removed from soils through the dissolution of Fe hydroxides (Smith et al. 1998) which supports this interpretation. These results were further supported by the geochemical modeling, which predicted As(III) was the dominant species under anoxic conditions. In the case that As species removed from the soil in anoxic conditions the As may also be attenuated by the iron coated sands that underlie the waste at the WMAF site which was further explored in the batch experiments. This attenuation of As(III) can happen within a pH range of 6-9 to the same extent as As(V) onto amorphous iron oxides and goethite, (Dixit and Hering, 2003).The sands underlying the waste are coated primarily by goethite and ferrihyrite, however because there is no spatial or depth trend in the concentration of the hydroxides it is difficult to predict where amorphous and crystalline hydroxides exist. This heterogeneity is problematic because the As species desorb from ferrihydrite more quickly, due to a weaker bond, than from the crystalline goethite. Although this adds complexity to the situation, it shows that there is potential for release of As into the groundwater system as was seen in the anoxic leaching experiment.

In the sequential extraction experiment the greatest concentrations of As were released in the strongly-sorbed fraction (F2) and the co-precipitated with amorphous Fe, Mn, and Al

hydroxides fraction (F4), which verifies that reductive dissolution would result in the release of As species into the groundwater system. The extractant used for the strongly sorbed fraction, NaH_2PO_4, has been known to release the majority of the As species in soil samples (Root et al., 2007). Similar results for the amorphous and poorly crystalline as well as the crystalline Fe-oxyhydroxide fractions have also been observed (Root et al., 2007). Because there was no final digestion performed the As that was sorbed in disulfide minerals would not be accounted for in the total amount of As that was released from the soil. The total percentages that were released from each sample were not as expected but this can be explained by the heterogeneity of the soil obtained from WMAF and the results mirror what would be expected at the site. Because of the heterogeneity different depths and geographical locations within the site would be expected to release varying levels of As.

The XRD results showed that the primary minerals present are quartz, calcite, k-spar, dolomite, anorthite, and iron oxides. The dominant As species was found to be As(V) which implies that sorbtion will be present and control the mobility of the As species in the system, this aligns with the results of the oxic system column experiment results. Arsenic can be incorporated into the crystal lattice or adsorbed to the surface of calcite (Renard et al., 2015 and Costagliola et al., 2013), dolomite (Stec et al., 2006 and Ayoub et al., 2007), and iron oxides (Smedley and Kinniburgh, 2002). It is likely that some of the arsenic species present are precipitated in these minerals. The possibility for release into the groundwater system will vary based upon the level of the water table, the competing ions present, the oxidation state of the system, and the pH of the system. The cracks in the cover will allow water to infiltrate into the waste and this will increase the allowance of As mobility in the system as seen by Onken and Hossner (1995) with flooding causing the release of As. Competing ions most commonly phosphate lessens the likelihood of the release As to be sorbed by the underlying iron coated sands, this is enhanced with greater infliltration (Dixit and Hering, 2003; Campos, 2002). The current state of WMAF will limit the mobility of As(V) species, however with increased infiltration due to the cover system failure As movement is possible.

Arsenic species are likely to be released under reducing conditions at near neutral pH conditions which are the usual pH conditions seen in groundwater systems. Under these conditions As(III) is present in neutrally charged complexes and does not sorb effectively allowing for mobility through the groundwater system. Iron oxyhydroxide coated sands much

like that underlying the waste at WMAF have been shown to sorb As species and limit their mobility through the groundwater system (Thirunavukkarasu and Viraraghavan, 2003; Mohan and Pittman, 2007; Arun and Chaudhuri, 1996). The sand underlying the waste has the potential to attenuate the As that is released from the waste however due to the inefficient sorption properties of As(III) in reducing conditions at near neutral pH and the thermodynamic stability, (Smith et al., 1998), As may not be effectively removed, a maximum of 35% of the As was attenuated on the underlying sand over 128 hours. Under oxidizing conditions As(V) can easily be sorbed by the underlying sands due to its oxyanion complexes at near neutral pH which can easily and strongly sorb to the Fe coated sand underlying the waste up to 100% of the As was sorbed by the underlying sand over 128 hours. Marin et al. 1993 and Thirunavukkarasu and Viraraghaavan, 2003 found these results to be true as well and suggested both species may be effectively removed from solution using Fe-oxide coated sands.

4.2. Uranium

Similar to As, the XANES data showed that U was present in both the U(IV) and U(VI) oxidation states at both locations where samples were obtained. This again reinforces the importance of the consideration of all possible conditions to determine contaminant transport of fate outcomes at WMAF. Uranium release was greatest under oxic conditions, where more mobile species U(VI) were predicted during geochemical modeling (Fein et al. 2013). Uranium(VI) is easily desorbed from Fe-oxides under oxic conditions and forms stable carbonate complexes that exhibit enhanced mobility (Zhou and Gu, 2005). Because these aqueous complexes are so stable at the pH of groundwater systems and in oxidizing environments it is unlikely that they would be easily resorb to the Fe-oxides the coat in the sands underlying the waste. The stability of the aqueous complexes is also likely to inhibit the reduction of the U species meaning the immobilization from sorption of U(IV) species or production of insoluble uraninite is not probably in oxidized systems (Zachara et al. 2007). Under anoxic conditions, U leaching was likely limited due to the strong sorption properties of U(IV) in reducing conditions as well as precipitation of highly insoluble UO_2. Sorption of the UO_2^{2+} ion is greatest between a pH of 6 and 7 which is characteristic of groundwater conditions (Hsi and Langmuir, 1985). These results were further supported through the PHREEQC model which showed the dominant species in oxic conditions was U(VI) and the dominant species in anoxic conditions was U(IV).

The model showed the under oxic conditions the U species can be liberated and enter the groundwater system.

The extractions showed that U could be released into the groundwater system at WMAF under certain conditions. The most substantial amounts of U were released in the strongly sorbed, co-precipitated with Fe, Mn, and Al hydroxides, and acid soluble fractions. Not all U would have been released because a final acid digestion was not performed, and it is possible that not a lot of U was sorbed initially in the waste. These results were not surprising and have been observed several times before and can easily be explained by the redox properties present and the pH of the system discussed above. (Milton and Brow, 1986; Hsi and Langmuir, 1985; Van der Weilden et al. 1976). The varying percentages released and the sample that released greater than 100% of the U that was determined present through the whole rock analysis can be explained by the heterogeneity of the waste at WMAF. Variations in contaminant concentrations should be expected at the site based upon depth and locations of the samples with no specific trends.

The XRD results showed that the primary minerals present are calcite, dolomite, and iron oxides. Uranium can be incorporated into the lattice or sorb to the surface of calcite (Bell, 1963 and Sturchio et al., 1998), dolomite (Bell, 1963), and iron oxides (Fein et al., 2013). It is likely that a significant portion of the U species present in the waste are contained in these minerals, however changes in infiltration, water table level, pH, and redox conditions can liberate these species.

Under oxidizing conditions U(VI) is likely to be mobile under the pH conditions from in groundwater systems, these findings were also seen by Hsi and Langmuir (1985) and Davis and Kent (1990). The batch experiments showed that U species can be sorbed by the underlying sand in both conditions, however if U is already present on the sand it may be released into the system likely because of competition for limited sorption sites. The reversibility of U sorption to underlying sands has been observed previously by Hsi and Langmuir (1985) and this can account for the variabilities that were seen in the batch experiment results. Under both anoxic and oxic conditions over 90% of the U species were attenuated by the sand underlying the waste.

4.3. Molybdenum

The XANES data showed that the dominant species of Mo at the WMAF is Mo(VI) as was expected. This further supports the importance of the pH controls at the site in relation to the transport and fate of Mo species. Molybdenum is controlled mainly by the pH conditions of a system, in the typical groundwater pH conditions seen at WMAF it is likely that Mo would be relatively mobile which has been observed several times in previous studies, (Jones 1957; Ferreiro et al. 1985; Goldberg et al. 2002). This was demonstrated in the column experiments where Mo movement was constant in both anoxic and oxic conditions throughout the entirety of the experiment plateauing only when the concentration of Mo was limited in the sample, not due to redox controls. Mo showed the potential to have a negative sorption onto the sand underlying the waste which may be due to the presence of Mo already having moved through the waste and being sorbed to the sand, and subsequently desorbing over time when exposed to water, this phenomenon was also seen by Ching-Kuo and Langmuir (1985) where the sorption was found to be variable and reversible. Mo also showed greater than 100% removal in the extraction experiment, this is likely due to the heterogeneity of the samples that were acquired at WMAF. The XRD data showed that the main minerals present in the soil were calcite, dolomite, anorthite, and iron oxides. Molybdenum sorbtion has been studied at length by Jones (1957) and it has been well established that Mo effectively sorbs to Iron oxide minerals. Under the current pH conditions of the WMAF Mo has the potential to move into the groundwater system.

CHAPTER 5. CONCLUSIONS

The collection of experiments performed showed results consistent with the literature and with the hypothesis of this project. This proves to be problematic because under any condition: reducing, oxidizing, and over a wide range of pH values, there is potential for contaminant movement from the waste into the underlying sand. The underlying sand has potential to attenuate some of the contaminant that moves, however the potential will change based up on the conditions, the amounts of contaminant present, and the sorption site competitors that are released into the system. Should infiltration occur, or the water table rise contaminants will enter the groundwater system. Under reducing conditions As and Mo have the potential to become mobile. Under oxidizing conditions U and Mo have the potential to become mobile.

The studies that were performed and the PHREEQC results showed that the contaminants at the WMAF will remain sorbed or be controlled by the iron coated sands to great enough extent that the contaminants will remain under the allowable limits for decades. The 1993 study that was performed concluded that remedial action should be taken eventually, however they suggested that the site could stay in its current state for at least one more decade. These results have proved to be accurate and supported by the current study, the site has not yet become and environmental hazard.

If conditions change at the WMAF site the likelihood of the contaminants, becoming mobilized increases. Because the water table changes significantly throughout the year there is opportunity for the contaminants to be liberated. If the water table depletes it is likely that U will have a higher likelihood of movement as the system becomes more oxidized. In the case that infiltration causes an increase in the water table the system will become more reduced and the As will be more likely to move into the saturated zone. Mo is likely to move at any pH that will be experienced in the aquifer in both reduced and oxidized states, thus Mo may be the most likely to move through the system to the saturated zone and toward the bulk storage swamp.

To minimize the potential of groundwater contamination repair of the current cover to prevent infiltration should be considered. There are a few options that could be considered to repair or replace this cover: using a geosynthetic cover or using a clay cover similar to the one in

place. A geosynthetic cover or additional clay cover would restrict gases and liquid from infiltrating the groundwater system allowing a stable environment for limited contaminant mobility. The current cover has cracks and has shown signs of infiltration into the waste, and there are signs of some movement of As, U and Mo into the underlying sands although they have not come near the water table yet.

CHAPTER 6. REFERENCES

Alam MS; Cheng T. Uranium Release from Sediment to Groundwater: Influence of Water Chemistry and Insights into Release Mechanisms, Journal of Contaminant Hydrology. 2014. 164, 72-87.

Anabar A. Molybdenum Stable Isotopes: Observations, Interpretations, and Directions, Reviews in Mineralogy and Geochemistry. 2004. 55, 429-454.

Appelo CAJ; Van Der Weiden MJJ; Tournassat C; Charlet L. Surface Complexation of Ferrous Iron and Carbonate on Ferrihydrite and the Mobilization of Arsenic, Environmental Science
and Technology. 2002. 36, 3096-3103.

Ayoub GM; Mehawej M. Adsorption of Arsenate on Untreated Dolomite Powder. Journal of Hazardouse Materials. 2007. 148, 259-266.

Banning A; Demmel T; Rude TR; Wrobel M. Groundwater Uranium Origin and Fate Control in a River Valley Aquifer. Environmental Science and Technology. 2013. 47, 13942-13948.

Barnett MO; Jardine PM; and Brooks SC. U(VI) Adsorption to Heterogeneous Subsurface Media: Application of a Surface Complexation Model, Environmental Science & Technology. 2002. 36, 937-942.

Bea SA; Wainwright H; Spycher N; Faybishenko B; Hubbard S; Denham M. Identifying Key Controls on the Behaviour of an Acidic-U(VI) Plume in the Savannah River Site using Reactive Transport Modelling. Journal of Contaminant Hydrology. 2013. 151, 34-54.

Bell KG. Uranium in Carbonate Rocks. Shorter Contributions to General Geology.1963. 474-A.

Bopp CJ; Lundstrom CT; Johnson TM; Sanford R; Long P; Williams K. Uranium U-235/U-238 Isotope Ratios as Indicators of Reduction: Results from an in Situ Biosimulation Experiment at Rifle Colorado, USA. Environmental Science and Technology. 2010. 44, 5927-5933.

Bostick BC Fendorf S. Differential Adsorption of Molybdate and Tertrathiomolybdate on Pyrite. Environmental Science and Technology. 2003. 37, 285-291.

Burton ED; Johnston SG; Kocar BD. Arsenic Mobility during Flooding of Contaminated Soil: The effect of Microbial Sulfate Reduction. Environmental Science and Technology. 2014, 48, 13660-13667.

Campbell KM; Kukkadapu KR; Qafoku NP; Peacock AD; Lesher K; Williams KH; Bargar JR; Wilkins MJ; Figueroa L; Davis AJ; Long PE. Geochemical, Mineralogical, and Microbiological Characteristics of Sediment from a Naturally Reduced Zone in a Uranium Contaminated Aquifer, Applied Geochemistry. 2012. 27, 1499-1511.

Costagliola P; Bardelli F; Benvenuti M; Di Benedetto F; Lattanzi P; Romanelli M; Paolieri M; Rimondi V; Vagelli G. Arsenic Bearing Calcite in Natural Tavernites: Evidence from Sequential Extraction, μXAS, μXRF. Environmental Science and Technology. 2013. 6231-6238.

Davis JA; Kent DB. Surface Complexation Modelling in Aqueous Geochemistry, Review Minerals. 1990. 23, 177-260.

Deschamps E; Ciminelli VST; Weidler PG; and Ramos A. Arsenic Sorption onto Soils Enriched in Mn and Fe Minerals, Clay and Clay Minerals. 2003. 51, 197-204.

Dixit S; Hering JG. Comparison of Arsenic(V) and Arsenic(III) sorption onto Iron Oxide Minerals: Implications for ArseNic Mobility, Environmental Science and Technology. 2003. 37, 4182-4189

Dong W; William PB; Chongxuan L; Zheming W; Stone AT; Bai J; Zachara JM. Influence of Calcite and Dissolved Calcium on uranium(VI) Sorption to a Hanford Subsurface Sediment. Environmental Science & Technology. 2005. 39, 7949-7955.

Edmunds WM; Smedley PL. Groundwater Geochemistry and Health: An Overview. Geological Society, London. 1996.

Elwakeel KZ; Atia AA; Donia AM. Removal of Mo(VI) as Oxyanions from Aqueous Solutions Using Chemically Modified Magnetic Chitosan Resins. Hydrometallurgy. 2009. 97, 21-28.

Erickson BE; Helz GR. Molybdenum(VI) speciation in Sulfidic Waters: Stability and Lability of Thiomolybdates, Geochimica et Cosmochimica Acta. 2000. 64, 1149-1158.

Ewing RC; Finch RJ. The corrosion of uraninite under oxidizing conditions. The Journal of Nuclear Materials. 1992. 190, 133-156.

Farquhar ML; Charnock JM; Livens FR; Vaughan DR. Mechanisms of arsenic uptake from aqueous solution by interaction with goethite, lepidocrocite, mackinawite, and pyrite: an X-ray absorption spectroscopy study. Environmental Science and Technology. 2002, 1757-1762.

Fein JB; Powell BA. Uranium adsorption: Speciation at Mineral-Water and Bacterial Cell-Water Interface. Mineralogical Association of Canada. 2013. 165-192.

Fendorf S; Herbel MJ; Kocar BM; Tufano KJ. Contrasting Effects of Dissimilatory Iron(III) and Arsenic(V) reduction and Arsenic Retention and Transport, Environmental Science and Technology. 2006, 40, 6715-6721.

Geng C; Jian X; Su Y; Hu Q. Assessing molybdenum adsorption onto an industrial soil and iron minerals, Water, Air, Soil, and Pollution. 224, 1743.

Giblin AM; Batts BD; Swaine DJ. Laboratory Simulation Studies of Uranium Mobility in Natural Waters. Geochimica et Cosmochimica Acta. 1981. 45, 699-709.

Goldberg S; Forster H; Godfrey C. Molybdenum Adsorption on Oxides, Clay Minerals and Soils, Soil Science of America. 1996. 60, 425-432.

Goldberg S; Forster HS. Factors Affecting Molybdenum Adsorption by Soils and Minerals. Soil Science. 1998. 163, 109-114.

Goldberg S; Lesch SM; Suarez DL. Predicting Molybdenum Adsorption by Soils Using Soils Chemical Parameters in the Constant Capacitance Model, Soil Science of America Journal. 2002. 65, 1836-1842.

Gražulis S; Chateigner D; Downs RT; Yokochi A; Quiros M; Lutterotti L; Manakova E; Butkus J; Moeck P; Le Bail A; Crystallography Open Database - an open-access collection of crystal structures. J. Appl. Crystallogr. 2009. 42, 726-729. https://dx.doi.org/10.1107/S0021889809016690

Gustafsson JP. Modelling molybdate and tungstate adsorption to ferrihydrite. Chem. Geol. 2003. 200, 105–115.

Helz GR; Bura-Nakic E; Mikac N; Ciglenecki I. New Model for molybdenum behavior in euxinic waters. Chem. Geol. 2011. 284, 323-332.

Hsi CD; Langmuir D. Adsorption of Uranyl onto Ferric Oxyhydroxides: Application of the Surface Complexation Site-Binding Model, Geochimica et Cosmochimica Acta. 1985. 49, 1931-1941.

Jakobsen R; Postma D; Pederson HD. Release of Arsenic Associated with reduction and Transformation of Iron Oxides, Geochimica et Comochimica Acta. 2006, 70, 4116-4129.

Javed MB; Kachanoski G; Siddique T. A Modified Sequential Extracion Method for Arsenic Fractionation in Sediments, Analytica Chimica Acta. 2013. 787, 102-110.

Jones FT; A Broad View of Arsenic, Poultry Science. 2007, 86, 2-14.

Jones LHP. The Solubility of Molybdenum in Simplified Systems and Aqueous Soil Suspensions, European Soil Science. 1957. 8, 313-327.

Joshi A; Chaudhuri M. Removal of Arsenic from Ground Water by Iron Oxide Coated Sand. Journal of Environmental Engineering. 1996. 8, 769-771.

Kinniburgh DG; Smedley PL. A Review of the Source, Behaviour and Distribution of Arsenic in Natural Waters, Applied Geochemistry, 2002. 17, 517-568.

Kirk MF; Holm TR; Park J; Jin Q; Sanford R; Fouke B; Bethke C. Bacterial Sulfate Reductions Limits Natural Arsenic Contamination in Groundwater, Geology. 2004. 32, 953-956.

Kirk MF; EE Roden; Crossey LJ; Brealey AJ. Experimental Analysis of Arsenic Precipitation During Microbial Sulfate and Iron Reduction in Model Aquifer Sediment Reactors, Geochimica et Cosmochimica Acta. 2010. 75, 2538-2555.

Kocar BD; Borch T; Fendorf S. Arsenic Repartitioning During Biogenic Sulfidization and Transformation of Ferrihydrite, Geochimica et Cosmochimica Acta. 2010. 74, 980-994.

Krupka KM; Serne RJ. Geochemical Factors Affecting the Behaviour of Antimony, Cobalt, Europium, Technetium and Uranium in Vadose Sediments. 2002.

Langmuir D. Uranium Solution-Mineral Equilibria at Low Temperatures with Applications to Sedimentary Ore Deposits, Geochimica et Cosmochimica Acta. 1978. 42, 547-569.

Langner P; Kretzchmar R; Marcus MA; Mikutta C; Suess TE. Spatial Distribution and Speciation of Arsenic in Peat Studied with Microfused X-ray Fluorescence Spectrometry

and X-ray Absorption Spectroscopy, Environmental Science and Technology. 2013. 47, 9706-9714.

Light TS; Standard for Redox Potential Measurements, Analytical Chemistry. 1972. 44(6), 1038-1039.

Longtin JP. Occurrence of Radon, Radium, and Uranium in Groundwater, American Water Works Association.1998. 80, 84-93.

Lowers HA; Breit GN; Foster AL; Whitney J; Vant J; Uddin MN; Muneem AA. Arsenic Incorporation into Authigenic Pyrite, Bengal Basin Sediment, Bangladesh, Geochimica et Cosmochimica Acta. 2007. 71, 2699-2717.

Marin A; Masscheleyn PH; Patrick WG. Solid Redox-pH Stability of Arsenic Species and its Influence on Arsenic Uptake by Rice, Plant and Soil. 1993. 245-253.

Mkandawire M. Biogeochemical Behaviour and Bioremediation of Uranium in Waters of Abandoned Mines, Environmental Science and Pollution Research. 2013. 20, 7740-7767.

Mohan D; Pittman CU. Arsenic Removal from Water/Wastewater Using Adsorbents- A Critical Review. Journal of Hazardous Materials. 2007. 142, 1-53.

Milton GM; Brown RM. Adsoprtion of Uranium from Groundwater by Common Fracture Secondary Minerals, Canadian Journal of Earth Sciences. 1987. 24, 1321-1328.

Nriagu J; Nam DH; Ayawola TA; Dinh H; Erdenechimeg E; Ochir C; Boloramaa T. High Levels of Uranium in Groundwater of Ulaanbaatar Mongolia. Science of the Total Environment. 2012. 414, 722-726.

Orloff KG; Mistry K; Charp P; Metcalf S; Marino R; Shelley T; Melaro E; Donhoe A; Jones R. Human Exposure to Uranium in Groundwater, Environmental Research. 2004. 94, 319-326.

Parks GA. The Isoelectric Points of Solid Oxides, Solid Hydroxides and Squeous Hydroxo Complex Systems, Chemical Reviews. 1965. 65, 177-198.

Parsons CT; Couture RM; Omeregie EO; Bardelli F; Grenche JM; Roman-Ross G; Chalet L. The Impact of Oscillating redox conditions: Arsenic Immobilization in Contaminated Calcareous Floodplain Soils. Environmental Pollution, 2013. 178, 254-263.

Qafouku NP; Gertman BN; Kukkadapu RK; Arey BW; Williams KH; Mouser PJ; Heald SM; Bargar JR; Janot N; Yabusaki S; Long PE. Geochemical and Mineralogical investigation

of uranium in multi-element contaminated, organic rich subsurface sediment. Applied Geochemitsry. 2014. 42, 77-85.

Ranville JF; Hendry MJ; Reszat TN; Xie Q; Honeyman B. Quantifying Uranium Complexation by Groundwater Dissolved Organic Carbon Using Asymmetrical Flow Field-Flow Fractionation. Journal of Contaminant Hydrology. 2007. 91, 233-246.

Ravel B; Newville M; ATHENA, ARTEMIS, HEPHAESTUS: data analysis for X-ray absorption spectroscopy using IFEFFIT. J. Synchrotron Radiat. 2005 12, 537-541. https://dx.doi.org/10.1107/S0909049505012719

Renard F; Putnis CV; Montes-Hernandez G; Ruiz-Agudo E; Hovelmann J; Sarrett G. Interactions of Arsenic with Calcite Surfaces Revealed by In Situ Nanoscale Imaging, Geochimica et Cosmicha Acta. 2015. 61-79.

Ressler T; Timpe O; Neisus T; Find J; Mestl G; Dieterle M; Schogl R. Time-Resoolved XAS Investigation of the Reduction/Oxidation of MoO_{3-x}' Journal of Catalysis. 2002. 67-83.

Root RA; Dixit S; Campbell KM; Jew AD; Hering JG; O'Day PA. Arsenic Sequestration by Sorption Processes in High-Iron Sediments, Geochimica et Cosmochimica. 2007. 5782-5803.

Savage KS; Tingle TN; O'Day PA; Waychunas GA; Bird DB. Arsenic Speciation in pyrite and secondary weathering phases, Mother Lode Gold District, Tuolume County, California, Applied Geochemistry. 2000, 1219-1244.

Smedley PL; Soruces and Distribution of Arsenic in Groundwater, In: Arsenic in Groundwater a World Problem. 2008, 4-32.

Smith ERG; Naidu R; Alston AM. Arsenic in the Soil Environment: A Review, Advances in Agronomy. 1998.

Stec K; Bobrowski A; Kalcher K; Moderegger H; Geossler W. Determination of Arsenic in Dolomites with a Simple Field Spectrometric Device. Microchimica Acta. 2006. 153, 45-49.

Thirunavukkarasu OS; Viraraghavan T; Subramanian K. Arsenic Removal from Drinking Water Using Iron Oxide Coated Sand, Water, Air, and Soil Pollution. 2003. 142, 95-111.

Thomas Jefferson National Accelerator Facility. http://education.jlab.org/itselemental/ele092.html. Accessed August 19, 2014.

Toby BH; Von Dreele RB; GSAS-II: the genesis of a modern open-source all-purpose crystallography software package. J. Appl. Crystallogr. 2002. 46(2), 544-549. https://dx.doi.org/10.1107/S0021889813003531

Van der Weijden CH; Arthur RC; Langmuir D. Sorption of Uranyl by Hematite: Theoretical and Geochemical Implications. Geological Society of America. 1976. 1152-1164.

Waite TD; Davis JA; Payne TE; Waychunas GA; Xu N. Uranium (VI) Adsorption to Ferrihydrite: Application of a Surface Complexation Model, Geochimica et Cosmochimica Acta. 1994. 58, 5465-5478.

World Health Organization. Water Quality Guidelines, Standards and Health. 2001.

Xie X; Johnson TM; Wang Y; Lundstrom CM; Ellis A; Xiangli W; Duan M; Li J. Pathways of Arsenic from Sediments to Groundwater in the Hyporheic Zone: Evidence from an Iron Isotope Study. Journal of Hydrology. 2014. 509-517.

Xu N; Braida W; Christodoulatos C; Chen J. A review of molybdenum adsorption in soil/bed sediments; Speciation, mechanism, and model applications. Soild and Sediment Contam. 2013. 22, 912-929.

Zachara JM; Iton E; Liu C. Reactive Transport of Uranyl Ion in Soils, Sediments, and Groundwater Systems. Mineralogical association of Canada. 2013. 255-289.

Zhou P; Gu B. Extraction of Oxidized and Reduced Forms of Uranium from Contaminated Soils: Effects of Carbonate Concentrations and pH, Environmental Science and Technology. 2005. 39, 4435-4440.

ZoBell CE. Studies on Redox Potential of Marine Sediments. Bulletin of American Association of Petroleum Geologist. 1946. 30(4), 477-513.

CHAPTER 7. APPENDICES

7.1. Figure A-1 Depth Profile of Area F (After WMAF 1993 Report)

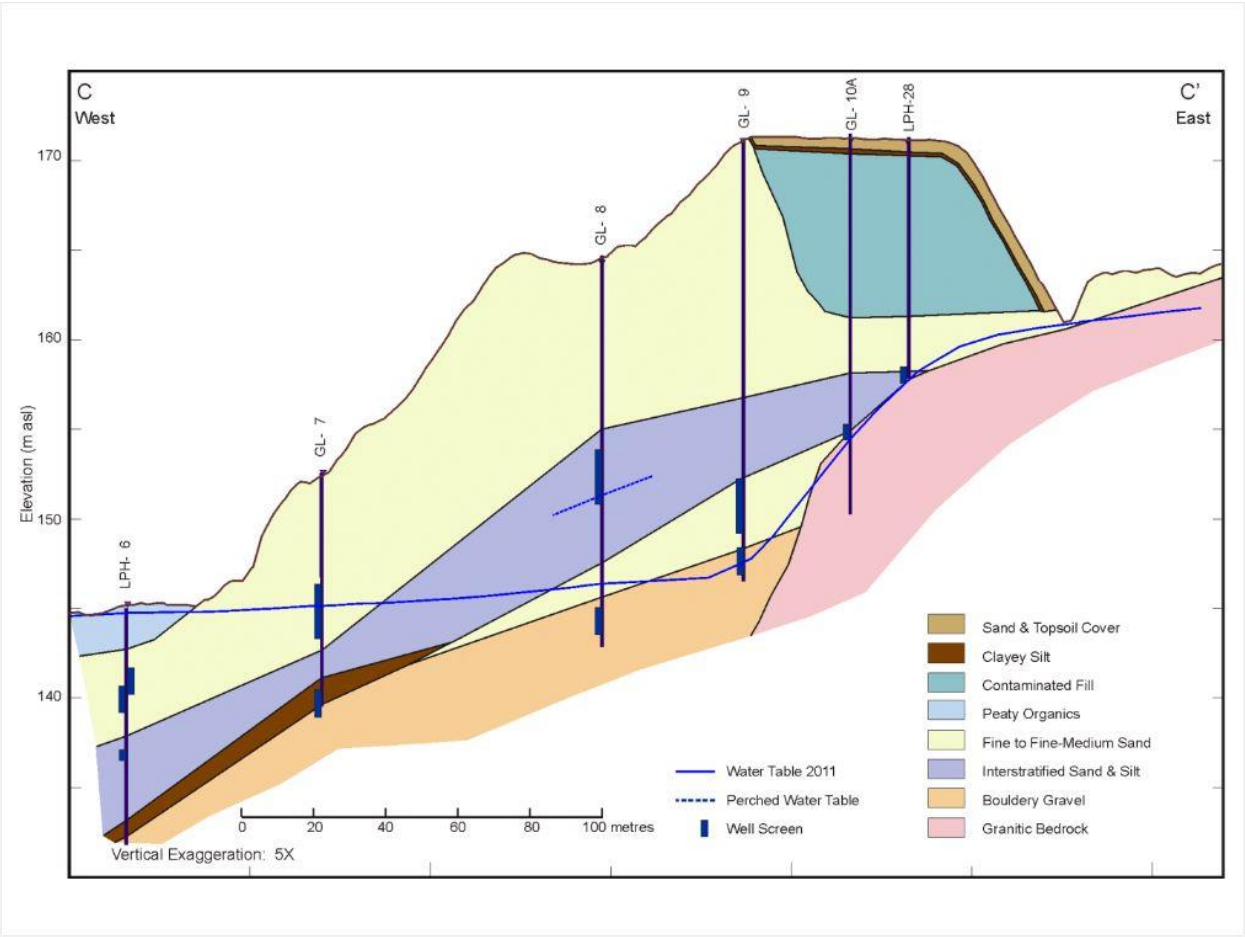

7.2. Figure A-2 Map of GL and LPH Series Boreholes at WMAF

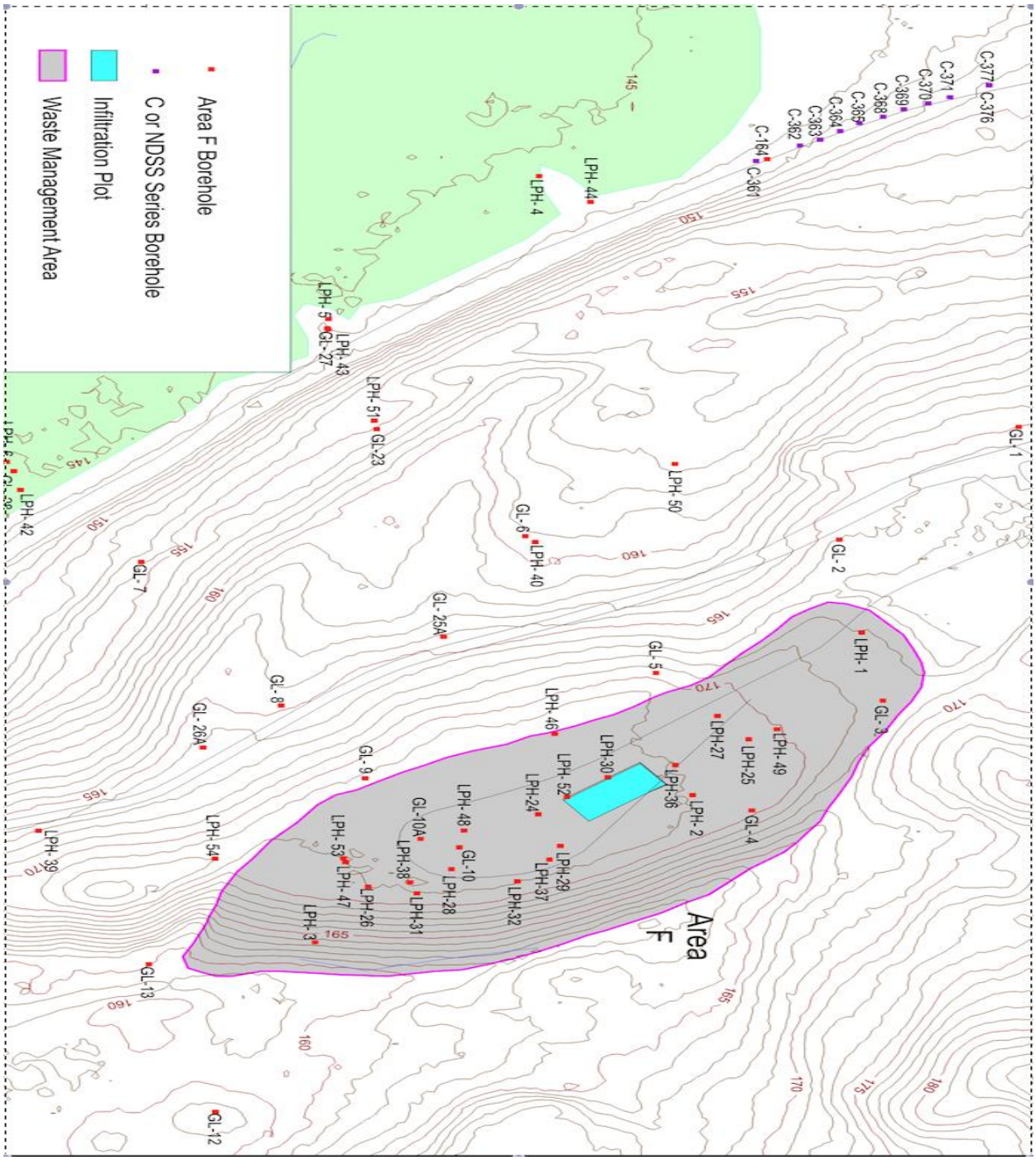

7.3. Figure A-3 Map from Gartner-Lee report 1977

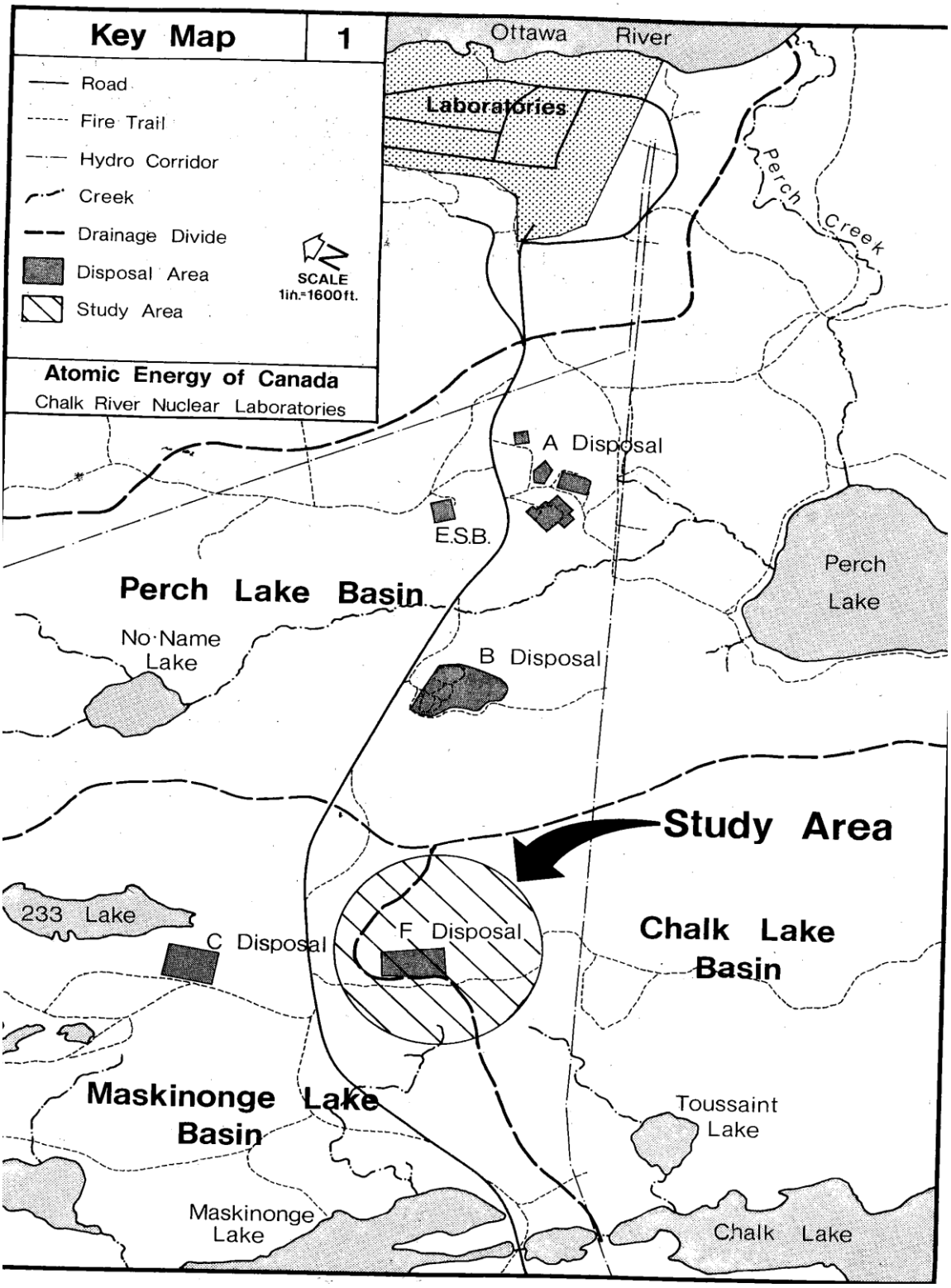

7.4. Table A- 1 Borehole Log from Sample Collection

Location	Date	Sample #	Sample Type	Depth (m)	Mass (g)	Lithology
LPH 49	25-Aug	1	spoon	6.86-6.93	794.06	Soil clay dark grey, iron staining
		2	core	6.93-7.37		sand very fine trace organics
		3	core	9.14-9.91		sand- fine
LPH 49a	26-Aug	1	spoon	.914-1.52		sand overlay clay coarse grain
LPH49-b	26-Aug	1 top	spoon	1.22-1.83	499.2	sand clay interface
		1 bottom	spoon	1.22-1.84	648	clay waste interface
LPH 52	26-Aug	1	spoon	0-0.12	182.04	sand, dirt, vegetation
		2	spoon	0.12-0.52	572.46	clay
		3	spoon	0.76-1.25	1003.08	sand coarse grain (interface to clay)
		4	spoon	1.25-1.31	201.17	clay (at interface from sand)
		5	spoon	1.52-1.798	572	clay with iron staining
		6	spoon	1.798-2.10	611.26	waste-brick wood, rock, black thick
		7	spoon	2.29-2.74	904.02	waste- brick rubber pebbles
		8	spoon	3.05-3.41	608.51	waste- wood, gray grains
		9	spoon	3.81-4.18	687.07	black waste
		10	spoon	4.57-5.09	1026.16	waste- iron, wood
		11	spoon	5.33-5.79	846.8	waste-iron
		12	spoon	6.096-6.43	563.78	black waste
		13	spoon	7.62-8.11	627.07	fine grain sand
	27-Aug	14	core	8.38-9.11		sand fine grain
		15	core	9.91-10.67		sand fine grain
		16	core	12.95-13.72		sand fine grain
LPH 53	28-Aug	1	spoon	0-0.24	350.32	organic, roots, coarse grain sand
		2	spoon	0.24-0.52	296.66	coarse sand
		3	spoon	0.76-1.07	397.5	fine grain sand(interface)
		4	spoon	1.07-1.22	316.74	clay-stiff grey (interface)
		5	spoon	1.52-1.59	95.23	clay (interface)
		6	spoon	1.59-2.07	746.68	black waste
		7	spoon	2.29-2.74	650.05	black waste
		8	spoon	3.05-3.54	927.95	black waste
		9	spoon	3.81-4.27	864.16	black waste
		10	spoon	4.57-5.06	778.28	black waste-wood, brick, asbestos
		11	spoon	5.33-5.79	886.63	black waste-cermanic, wood
		12	spoon	6.096-6.55	793.1	black waste

		13	spoon	6.86-7.04	258.25	black waste
		14	spoon	7.62-8.05	691.34	black waste
		15	spoon	8.38-8.87	785.66	black waste-brick
		16	spoon	9.14-9.6	875.8	black waste
		17	spoon	9.91-9.97	104.6	waste (interface)
		18	spoon	9.97-10.45	691.79	sand (interface)
		19	core	10.67-11.43		sand
		20	core	12.19-12.95		sand
	29-Aug	21	core	15.24-16.0		sand
		22	core	18.29-19.05		sand
		23	spoon	19.8-20.21	634.41	till
		24	spoon	20.57-21	766.26	silty sandy till
		25	spoon	21.34-21.64	446.57	silty sandy till

TOTAL SAMPLE MASS: **22704.66**

***All core samples have a volume of 94.25 in^3**

7.5. Table A-2 Column pH, Eh, and alkalinity data

Week	Parameter	LPH52-6a	LPH52-9a	LPH52-12a	LPH53-6a	LPH53-9a	LPH53-12a	LPH52-6b	LPH52-9b	LPH52-12b	LPH53-6b	LPH53-9b	LPH53-12b
1	pH	7.72	9.54	8.54	7.81	7.96	8.54	8.17	9.14	8.56	7.77	7.90	8.62
	Eh	-186.00	-37.30	-313.20	-496.00	-53.30	-418.70	186.20	96.50	161.00	190.00	163.80	135.30
	Alkalinity (mg/L)	145.63	239.23	104.76	39.22	40.82	70.28	62.37	334.68	122.00	58.82	64.13	111.34
2	pH	8.09	9.05	8.00	7.58	7.50	7.98	7.91	9.15	8.42	7.89	8.02	8.32
	Eh	-258.80	-91.50	-319.30	-182.70	-200.30	-218.40	169.80	121.90	159.80	178.90	178.30	177.30
	Alkalinity (mg/L)	267.33	368.93	301.89	310.00	270.83	241.07	122.45	119.88	173.08	98.62	121.09	160.32
3	pH	7.41	8.38	7.81	7.62	7.48	7.76	8.13	9.20	8.40	8.03	7.84	8.62
	Eh	-205.50	38.90	-156.90	-248.20	-221.70	-190.50	138.30	116.70	132.90	148.50	159.40	151.90
	Alkalinity (mg/L)	225.49	355.73	271.32	248.80	269.73	342.13	100.60	125.00	130.26	76.92	86.54	118.23
4	pH	7.62	8.36	7.84	7.46	7.50	7.76	8.04	9.13	8.48	8.24	7.92	8.85
	Eh	-178.40	-5.10	-146.00	-190.50	-139.40	-103.40	123.60	106.90	142.30	140.50	156.10	134.00
	Alkalinity (mg/L)	166.67	223.35	227.98	149.55	218.91	150.00	89.73	188.68	116.73	68.56	99.21	104.28
5	pH	7.76	8.24	7.77	7.53	7.55	7.61	8.17	9.07	8.45	8.13	8.12	8.86
	Eh	80.00	99.30	-85.00	-132.00	6.10	-127.60	217.90	128.40	151.90	139.70	195.80	138.70
	Alkalinity (mg/L)	110.00	159.52	126.21	84.51	78.82	160.00	69.86	116.28	89.02	72.54	94.34	98.04
6	pH	7.68	8.21	7.98	7.61	7.76	7.76	8.55	9.58	8.77	8.55	8.36	9.11
	Eh	-204.80	77.00	9.30	-105.40	-112.50	-117.80	90.90	95.10	198.40	114.30	119.40	117.20
	Alkalinity (mg/L)	128.08	133.33	97.09	84.27	79.52	125.97	50.66	149.53	79.37	74.23	61.22	88.06
7	pH	7.70	8.06	7.87	7.56	7.53	7.74	8.44	9.05	8.50	7.95	8.32	8.79
	Eh	-209.70	47.00	-92.50	-164.00	-148.00	-63.00	116.90	135.90	128.50	118.60	125.60	138.70
	Alkalinity (mg/L)	85.71	84.11	89.29	82.90	74.07	110.00	89.73	125.00	94.88	77.22	1.16	117.07
8	pH	7.70	8.04	7.90	7.64	7.60	7.77	8.38	8.97	8.12	8.29	8.29	9.07
	Eh	-72.30	124.10	68.60	-177.00	-127.20	-58.00	196.80	142.50	163.30	174.10	164.80	149.40
	Alkalinity (mg/L)	68.63	115.94	93.90	85.55	74.21	89.82	85.07	78.20	103.97	66.41	95.06	76.05
9	pH	7.75	8.03	7.96	7.71	7.66	7.77	8.43	8.74	8.23	8.25	8.14	9.00
	Eh	-226.90	75.60	-157.80	-181.90	-178.20	-146.70	225.90	179.30	175.20	174.90	175.10	172.40
	Alkalinity (mg/L)	98.81	79.52	102.04	88.76	82.64	90.00	69.58	92.34	96.71	60.24	77.07	74.07
10	pH	7.78	8.00	7.84	7.48	7.50	7.79	8.33	8.43	8.29	8.07	8.27	8.72
	Eh	-149.00	6.00	-155.00	-138.00	-122.00	-128.70	142.10	137.40	155.90	141.60	154.10	159.10
	Alkalinity (mg/L)	168.14	131.58	126.13	105.26	78.26	127.12	67.44	97.75	118.23	68.09	68.63	107.21
11	pH	8.78	7.95	7.83	7.47	7.54	7.84	8.07	8.33	8.05	8.11	8.01	8.26
	Eh	155.00	170.80	16.40	163.10	168.40	186.80	240.00	167.70	160.00	144.00	151.60	153.40
	Alkalinity (mg/L)	68.63	92.31	94.52	71.43	96.15	91.84	130.43	122.81	101.69	127.27	158.33	193.55
12	pH	8.17	8.50	8.08	7.94	8.00	8.07	8.02	8.11	7.81	8.01	8.00	8.01
	Eh	249.00	209.70	234.40	233.90	217.20	227.00	148.50	140.10	136.30	140.00	150.01	150.02
	Alkalinity (mg/L)	61.17	84.41	90.73	60.61	70.72	77.38	123.81	137.25	113.21	130.00	140.28	109.09
13	pH	7.88	8.43	8.14	7.90	7.80	8.00	7.99	8.23	8.04	8.06	8.04	8.22
	Eh	167.20	149.40	166.20	158.90	178.50	182.60	194.30	157.00	14.70	7.10	16.00	24.90
	Alkalinity (mg/L)	58.35	61.75	77.59	52.58	58.55	63.03	102.61	117.87	119.66	122.72	104.11	148.00
14	pH	8.04	8.35	8.08	7.99	7.88	8.14	7.90	7.89	8.00	7.94	7.85	8.19
	Eh	162.20	162.40	152.30	166.40	159.80	173.40	144.30	134.40	156.00	143.40	138.80	165.30
	Alkalinity (mg/L)	55.81	49.80	119.88	38.35	27.45	29.85	87.35	95.90	84.31	99.04	80.76	129.52
15	pH	8.49	8.74	8.37	8.26	8.13	8.44	7.99	8.07	7.93	7.84	7.72	7.76
	Eh	128.00	128.80	142.00	149.20	163.00	164.40	118.10	138.30	84.00	66.90	80.00	137.40
	Alkalinity (mg/L)	91.81	88.00	87.04	86.05	74.26	91.65	92.37	103.96	118.74	110.06	107.44	134.17
16	pH	8.32	8.54	8.25	8.00	8.00	8.08	7.98	8.25	8.11	8.13	7.98	8.13
	Eh	184.60	169.80	143.20	184.30	187.50	171.60	89.00	41.50	-111.50	-115.30	-84.10	68.00
	Alkalinity (mg/L)	96.74	90.18	86.91	88.78	71.43	93.88	96.74	114.37	143.00	154.63	94.74	148.04
17	pH	8.09	8.13	7.94	8.00	7.96	8.06	7.82	7.89	7.44	8.00	7.88	7.97
	Eh	248.60	180.30	208.90	212.50	232.90	193.80	-94.20	101.10	-125.00	140.00	98.50	100.00
	Alkalinity (mg/L)	68.49	53.55	120.71	30.30	98.04	89.11	106.21	116.77	150.20	126.92	115.58	166.84
18	pH	7.85	7.72	6.89	7.47	7.61	7.87	8.14	8.27	8.09	8.26	7.99	8.37
	Eh	132.80	139.10	134.80	161.90	164.40	169.00	102.20	126.30	50.80	76.80	126.30	106.80
	Alkalinity (mg/L)	72.14	74.78	81.00	65.26	65.07	80.12	61.90	48.08	70.71	26.04	30.00	48.08
19	pH	7.70	8.27	7.96	8.05	8.19	8.15	7.90	8.24	8.10	7.94	7.96	7.76
	Eh	129.00	154.20	164.80	166.40	166.40	173.10	-151.40	-54.30	-118.40	30.00	90.02	24.00
	Alkalinity (mg/L)	71.22	86.00	96.00	67.93	84.92	91.00	92.52	99.70	93.81	124.74	102.70	110.11
20	pH	7.32	8.15	7.94	7.76	7.98	8.01	7.60	8.24	8.29	7.98	8.12	8.52
	Eh	105.20	123.70	162.80	165.00	162.50	160.40	-173.50	-168.40	-90.30	-85.20	63.60	-86.30
	Alkalinity (mg/L)	86.00	89.46	103.90	27.97	80.76	101.39	82.62	85.17	88.38	121.78	84.06	102.68